Departement MTM
Metaalkunde en
Toegepaste Materiaalkunde

KATHOLIEKE
UNIVERSITEIT
LEUVEN

INVESTIGATION OF TEXTURE AND RESIDUAL STRESS AFTER COLD ROLLING OF SHEET METAL

ERASMUS THESIS PROJECT

Promotor:

Prof. dr. ir. Marc Seefeldt

By Álvaro Donoso Parrado

Supervisor:

Dr. ir. Koen Decroos

Academic year 2011 - 2012

CONTENT

1 Objective....4

1.1 Focus of this thesis....4

2 Introduction....4

2.1 Crystalline solid material....4

2.2 Rolling process....6

2.2.1 Definition....6

2.2.2 Cold rolling....8

2.2.3 Cold rolled sheet metal....8

2.2.4 Flow modeling....9

3 Texture in rolling processes....12

3.1 Introduction....12

3.1.1 Orientation of a single crystal....13

3.1.2 Orientation Distribution Function (OFD)....14

3.2 Pole Figures....14

4 Residual stress....16

4.1 Introduction....16

4.2 Stress strain behavior....16

4.3 Measured of residual stress....18

4.3.1 X-Ray Diffraction Method....19

4.3.2 Obtained stresses from strains....20

5 Crystal Plasticity Models....20

5.1 Theory of plasticity....20

5.2 Single crystal plastic behavior....21

5.3 Polycrystal plastic behavior....23

5.4 Taylor model....24

5.5 Alamel model....24

5.6 Visco-plastic self consistent model....24

5.7 Input parameters for crystal plasticity models....25

5.7.1 Velocity gradient and deformation gradient tensor.....25
5.7.2 Initial texture.....26
5.7.3 Monocrystal data.....26

6 Computational: fast material model.....27
6.1 Fast implementation of the material law predicted.....27
by crystal plasticity models: database principle
7 Results.....29
7.1 Taylor factor.....29
7.2 Texture.....30
7.3 Plastic anisotropy.....30
8 Calibration of the single crystal parameters.....31
8.1 Single crystal behavior.....31
8.2 Critical resolved shear stress.....38
8.3 Strain rate sensitivity.....40
8.4 Back extrapolated CRSS.....42
8.5 Asymptotic hardening rate.....44
8.6 Macroscopic behavior.....46
8.7 Conclusion.....47
9 General conclusions.....48
10 References.....49

1 OBJECTIVE

1 FOCUS OF THE THESIS

The purpose of this thesis is to study and measure the residual stresses and crystallographic texture induced by cold rolling processes of DC01 and DC04 steels.

The Visco Plastic Self Consistent (VPSC) model is a well established model for predicting the texture development and the mechanical behavior of a polycrystalline material. A key issue to use such a model is to know the single crystal plastic parameters. The aim of current work is to find these parameters in order to make a given experimental macroscopic strain-stress curve correspond as much as possible with the one predicted by a VPSC model. Considering that its plastic response on the grain level is described by al Voce hardening law, the influence of the initial critical resolved shear stress (τ_0), the back extrapolated critical resolved stress (τ_1), the asymptotic hardening rate (θ_0) and the inverse of the rate sensitivity (n) are studied.The manually obtained results are the initial values that can be used as an input for direct search simplex optimization algorithm in order to find the optimal values.

Once the parameters are known they can be used in a polycrystal plasticity model, in our case VPSC, to calculate the evolution of texture, anisotropy and hardening in any kind of deformation process. Current research was in support of a model to implement material anisotropy in fast models of cold rolling processes.

Due to a lack of time no residual stress measurements in cold rolled plates could be made.

2 INTRODUCTION

2.1 CRYSTAL SOLID MATERIAL

Solids exist in nature in two principal forms: crystalline and non-crystalline or amorphous, which differ substantially in their properties .In the amorphous state the elementary particles

are intermixed in a disorderly manner; there are not fixed relative to those of their neighbors. Crystalline bodies are characterized by an ordered arrangement of their ions, atoms or molecules. Most crystalline solids are made up of millions of tiny single crystals called grains. These materials are said to be polycrystalline.

A single crystal is symmetrical about its certain elements like points, lines or planes; this characteristic is based on the internal structure of the crystal and helps one to classify crystals and to describe their behavior. It is convenient to imagine points in space about which these atoms, ions or molecules are located. Such points in space are called lattice points, the total of lattice point form a space lattice, defined as an array of imaginary points which are arranged in space such that each point has identical surroundings. To obtain a crystal structure an atom or group of atoms must be placed on each lattice point in a regular way. Such an atom or a group of atoms is called the basis .A lattice combined with a basis generates the entire crystal structure .Whereas a lattice is a mathematical concept; the crystal structure is a physical concept. The smallest component of the space lattice is called “unit cell” which can be completely described by three vectors, and reflects the crystal’s symmetry.

There are several types of the lattices in which metallic atoms can arrange themselves upon solidification, but the three most common are shown in Figure 2.1 and are known as the body-centered cubic (BCC), which have an atom at each corner and one at the body centre ,face-centered cubic (FCC), and close-packed hexagonal (CPH) crystal lattices. (Material Science s.f.).

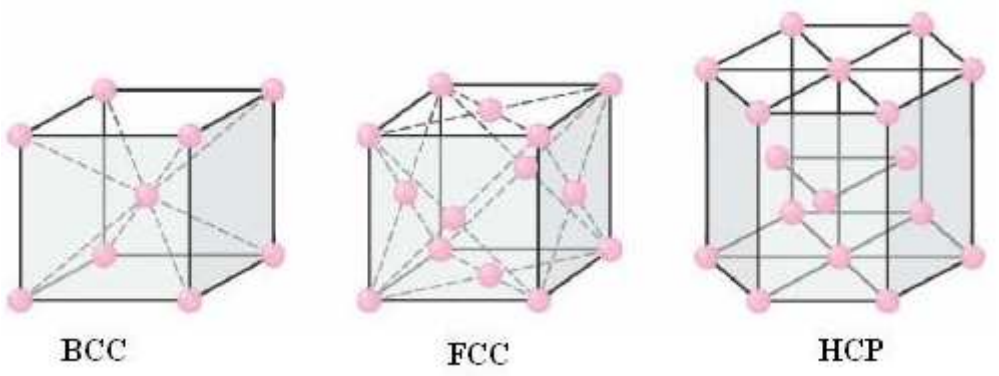

Figure 2.1 Three principal types of crystal lattices

The crystal lattice may be regarded as make-up of an aggregate of a set of parallel equidistant planes, passing through the lattice points, which are known as atomic planes. For a given lattice, one can choose the lattice planes in different ways. These crystal planes and crystal directions play an important role in hardening, plastic deformation and other properties.

One can determine the crystal structure by X-Ray Diffraction. When X-rays interact with a crystalline substance one gets a diffraction pattern as will be explained later.

In crystalline solids the atoms or molecules are stacked in a regular manner; forming a three-dimensional pattern which may be obtained by a certain pattern unit called unit cell. When the periodicity of the pattern extends throughout a certain piece of material, one speaks of a single crystal. Most single crystals exhibit anisotropy, which is, the presence of a variation of some physical properties according to the direction along which they are measured.

The mechanical behavior of crystalline materials is strongly influenced by microstructural properties such as crystallographic texture and grain structure.

It is possible to draw several sets of parallel planes through a crystal so that all atoms constituting it would be located in any one set. They are known as the atomic planes.

Figure 2.2 illustrates the atomic planes in a cubic cell which may be considered as made up of eight atoms, one at each corner. The atomic planes are described by the three-digit numbers. Each digit corresponds to a unit coordinate in relation to the crystallographic axes X, Y and Z.

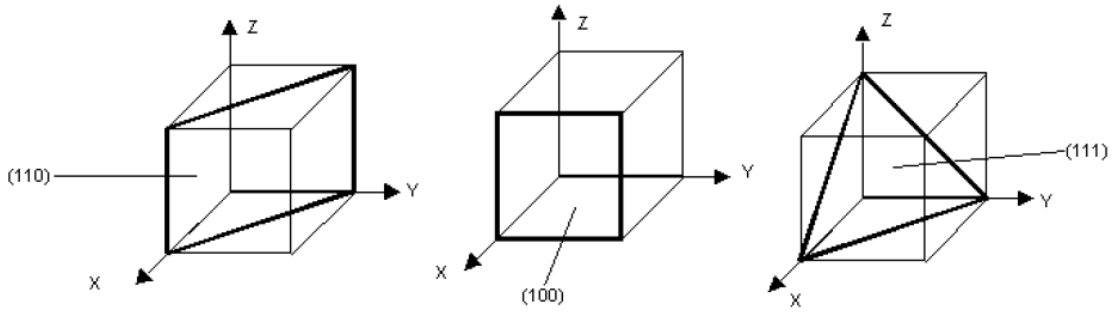

Figure 2.2 Atomic planes in a cubic cell

Physical properties as crystallographic anisotropy depend on the direction of their measurement in respect to their crystallographic axes. In the body-centered cubic crystalline structure, the greatest strength lies in the direction of the atomic plane (111) and the weakest along the atomic plane (100).

2.2 ROLLING PROCESS

2.2.1 DEFINITION

A rolling process is defined as the reduction of the thickness or changing cross-sectional area of the metal stock, or the general shaping of the metal products by compressive forces applied through a set of opposed rotating rolls. The rolls rotate as illustrated in Figure 2.3(b) to pull and simultaneously squeeze the work piece between them. (Neutron Diffraction Study of the Residual Stress State of a Cold-rolled Steel s.f.).

Figure 2.3(a) shows schematically the material´s development throughout the process. The material, with initial thickness h_o undergoes a change after the roller decrease the thickness to h_f due to the pressure exerted by the rollers on the material associated with the rolling force F.

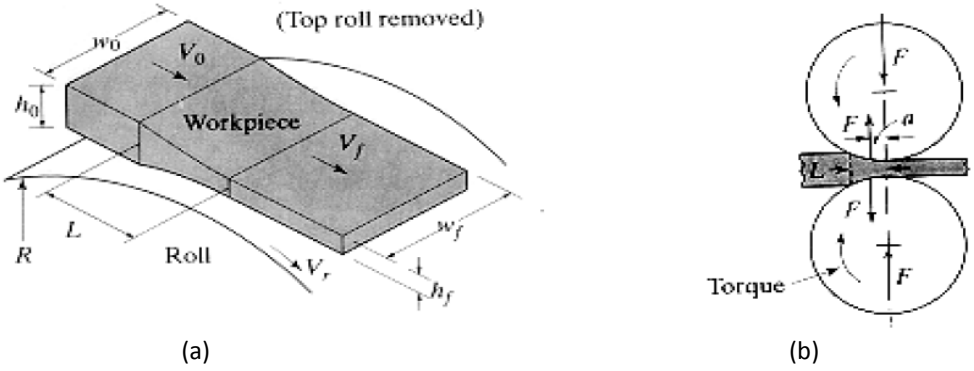

(a) (b)

Figure 2.3 (a) Schematic representation of rolling process. (b) Rolling force and torque

Due to the reduction in the section, the speed increases from V_0 to V_f during the process. As the superficial velocity in the rollers is constant (V_R), slip will be produced between the material sheet and the rollers along the arc of contact L. In the single point of contact called neutral or non-slip, the material velocity is equal to the surface speed of the roller. The rollers move faster than the material at the left of this point and lower on the right. These differences in the velocity produce frictional forces in opposite directions.

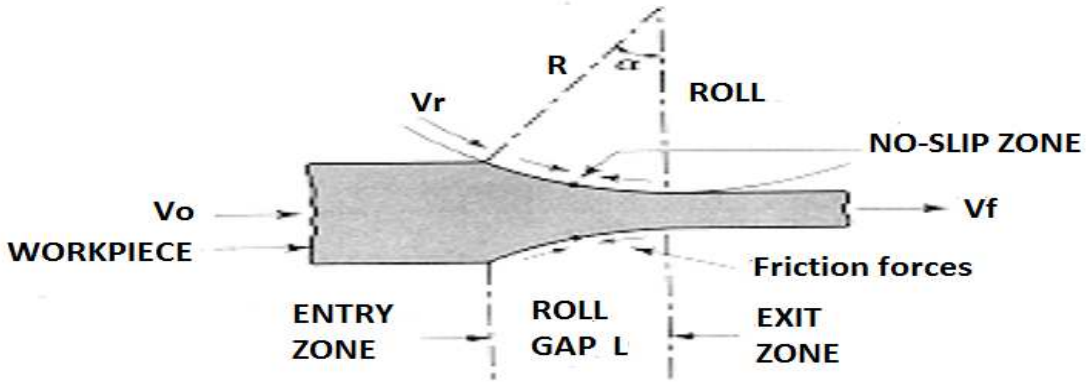

Figure 2.4 Frictional forces in lamination process

Figure 2.4 shows the effect of frictional forces appearing on the material during the rolling process. The resultant friction forces the material between the rollers against the resistance present in the material to avoid deformation. The frictional force produced to the left of the neutral point is bigger than the force corresponding to the right area.

Both, the force material which resist the entry of the material between the rollers, as well as, the resultant friction force will be increased proportionally to the thickness reduction in the process (h_0-hf).

The primary objectives of the rolling process are to reduce the cross-section of the incoming material while improving its properties and to obtain the desired section at the exit from the rolls. The process can be carried out hot, warm or cold, depending on the applications and the material involved. Sheet often is rolled cold in order to maintain close thickness tolerances.

2.2.2 COLD ROLLING

Cold rolling in the everyday sense means rolling at room temperature and without preheating, although the work of deformation can raise temperatures to 100-200 °C. Cold rolling usually follows hot rolling. A material subjected to cold rolling improves and refines the metallurgical properties of the metal and gives an excellent finish and accuracy. Still, there are disadvantages such as work hardening which increases further machining difficulties and pressing the unwanted internal stress inside the material surface which can cause unexpected distortion later, dislocation density increases, and when a tension test is performed on this strain-hardened material a higher stress will be needed to initiate and maintain plastic deformation, thus the residual stress increase. However, the ductility of the material drops because of the higher initial dislocation density.

2.2.3 COLD ROLLED SHEET METAL

The most common process for manufacturing cold rolled begins with a hot rolled coil pickling to obtain a clear surface to let free of oxides and inlays, subsequently passing through a

tandem train, where the thickness is reduced. Then the coils are subjected to a heat treatment or annealing, which may be continuous or bell, in order to regenerate the crystalline structure destroyed in the lamination process.

The DC04 is a cold-rolled low carbon steel, typically used for deep drawing applications. Its chemical composition is shown in Table 2.1. Such products are used in many fields of application in industry due to its versatility: the auto industry, the manufacture of metal furniture, white goods, etc…

Chemical composition of DC04

Element	C	Si	Mn	P	S	Al
max. wt%	0.08	-	0.4	0.03	0.03	-

Table 2.1

DC04 steel is obtained by cold forming which favors the characteristics of ductility and deformation or resistance qualities.

As an example, the microstructure and texture of DC04 steel from reference (Experimental identification and validation of models in micro and macro plasticity s.f.) is discussed. The specimen stem from a sheet with a thickness of 0.8 mm, the microstructure of which is shown in Figure 2.5. The grains exhibit a relatively small morphological texture with a mean grain size of 19 and 13 microns in rolling and transversal direction, respectively.

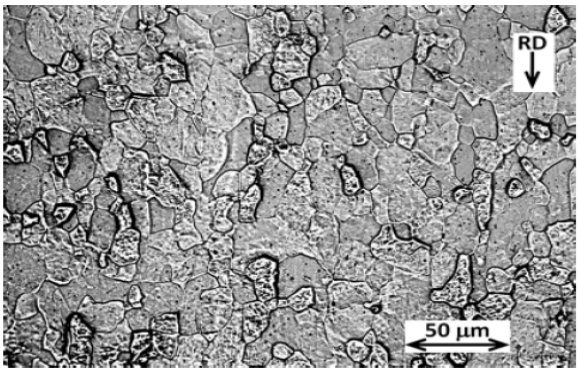

Figure 2.5: Microstructure of a DC04 steel sheet with 0.8 mm thickness (Experimental identification and validation of models in micro and macro plasticity s.f.)

2.2.4 FLOW LINE MODELING

In order to predict the development of material flow, a simple analytical flow function has been used in this work. The predicted velocity gradient resulting from this model can be used as an input into crystal plasticity models, like Taylor, Alamel and VPSC, which will be explained later.

In a rolling process, the material flows along certain flow lines, as can be seen in Figure 2.6. This makes sense, since in rolling processes of metals, no turbulence occurs. Beausir et al. proposed a method to calculate the velocity and consequently also the velocity gradient tensor, based on the assumption that in steady state the flow lines are know in advance (B. Beausir L. T., 2005).

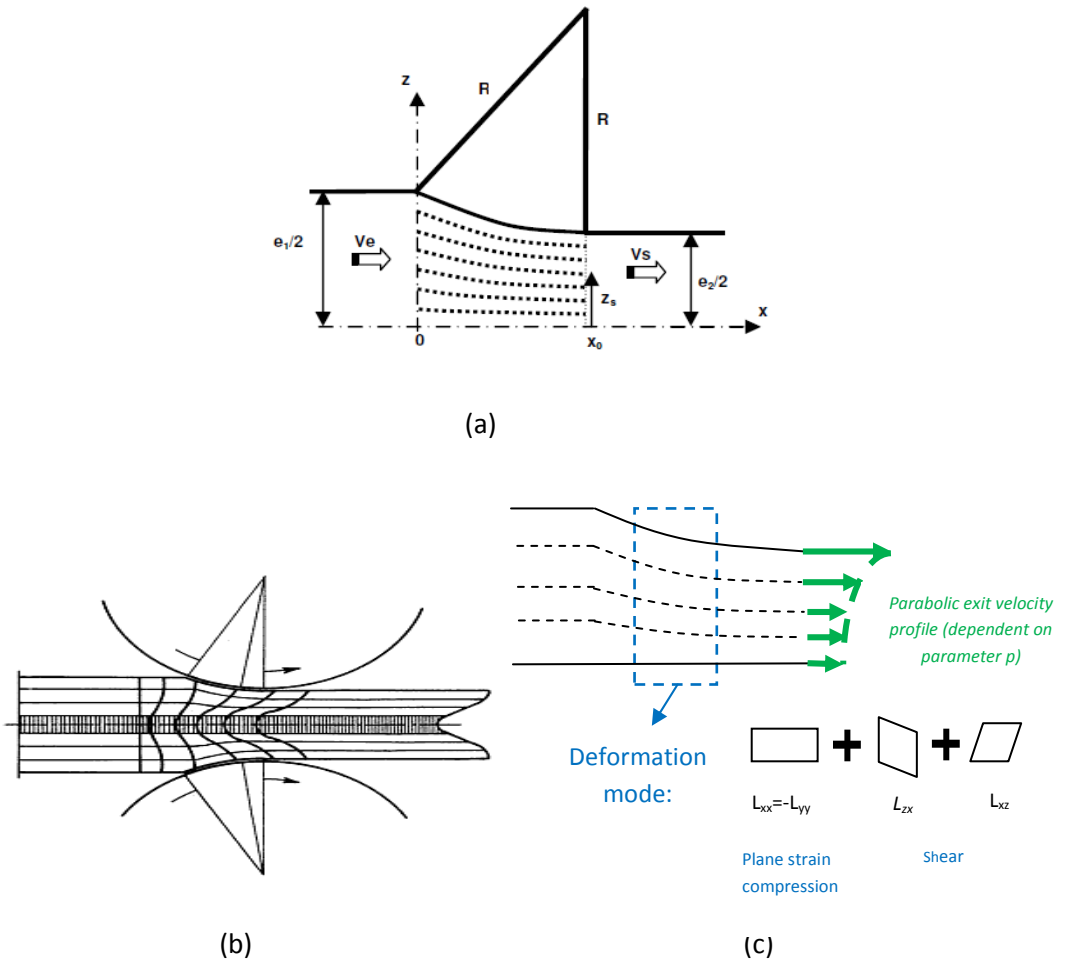

Figure 2.6: the principles of a flowline model. (a): the geometry parameters. (b): rolling process showing a difference in through thickness material flow. (c): schematic representation of the deformation modes, and the parabolic exit velocity profile.

As can be understood from Figure 2.6(b), depending on the friction conditions, the exit velocity also varies along the thickness of the plate. Beausir et al. stated that the flow lines have a mathematical equation, and the exit profile is parabolic over the thickness, depending only on one parameter, which is related to the friction between the rolls and the plate. For the geometry of Figure 2.6(a), the equation of one flow line is parabolic and given by the function 2.1 and 2.2:

$$\Phi(x,z)=\frac{z}{D(x)}=Cste \tag{2.1}$$

With

$$D(x)=\alpha+\beta(x-x_0)^2,\alpha=\frac{e_2}{e_1},\ \beta=\frac{1-\alpha}{x_0^2},\ x_0^2=R(e_1-e_2)-\frac{(e_1-e_2)^2}{4} \tag{2.2}$$

Based on this equation, the steady state regime, and the parabolic velocity exit profile, an analytical straightforward equation for the velocity gradient tensor can be found, based on the rolling parameters and one friction parameter.

As is schematically shown Figure 2.6(c), in rolling processes, the deformation mode is not only a plane strain compression as some authors assume, but is a combination of plane strain compression, and two types of simple shear. Online at mid thickness, the plane strain compression mode is valid. This has a clear effect on the through thickness texture evolution, as will be shown later.

As can be understood from the straightforward character, this method is very fast in calculating the velocity gradient and this at any point in space.

In this work, a more sophisticated model than equation 2.1 and 2.3 are used (B. Beausir L. T., 2009).

3 TEXTURE IN ROLLING PROCESS

3.1 INTRODUCTION

In a polycrystalline material each grain normally has a crystallographic orientation different from that its neighbors. If the orientation of all grains tends to cluster about some particular orientations, the material is said to have crystallographic texture. Radiation which is diffracted

by crystallographic lattice planes is able to provide information on their arrangement and consequently, on the orientation of the sampled volume of material with respect to some fixed reference axes.

One of the most important changes that can occur during a polycrystalline material forming process is the formation of new textures. The texture study is based on the calculation of the volume fraction associated with all orientations. Traditionally, the texture determination is performed using macroscopic techniques such as X-ray diffraction that allows studying the crystal orientation of a large number of grains and obtaining a statistical description of the macrotexture.

When the material with a deformation texture is recrystallized, the new grain structure may have a different texture from the deformation texture. After manufacturing processes such as cold rolling sheet metals there is often significant plastic anisotropy .For metals, the primary source of plastic anisotropy up to moderately large strains comes from the texture or the preferred crystallographic orientations of the grains. Consequently, the material properties are anisotropic so they may depend on the direction in which they are measured. The anisotropic behavior of polycrystalline materials may depend on the size, shape, crystallographic orientation, and arrangement of the crystals.

3.1.1 ORIENTATION OF A SINGLE CRYSTAL

The most common way to represent a crystal´s orientation is show in Figure 3.1.

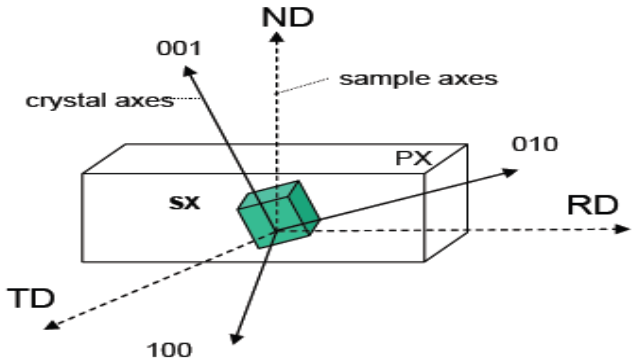

Figure 3.1 Representation texture

Three parameters describe the orientation of crystal axes with respect to samples axes. A usual choice are the three Euler angles $\varphi_1, \phi, \varphi_2$ as we can see in Figure 3.2.

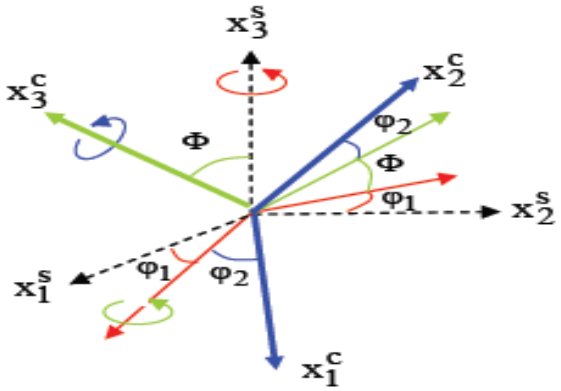

Figure 3.2 Euler angles

3.1.2 ORIENTATION DISTRIBUTION FUNCTION (ODF)

It is possible to represent texture as analytical combination of Euler angles. The Orientation Distribution Function (ODF) f(φ_1 ,ϕ , φ_2) gives the density of grains having a particular orientation φ_1 ,ϕ , φ_2 .The OFD is usually represented as intensity lines in 2D section in Euler spaces.ODF can be obtained from X-ray pole figures or from automated EBSD (electron backscattering diffraction).

The OFD statistically describe the texture or preferred orientation and is the keystone of texture analysis.

A typical texture analysis consists of the measurement of a sufficient number of pole figures, which depend on the crystal structure of the investigated materials, and subsequently an orientation distribution function (OFD) is calculated.

3.2 POLE FIGURES

Pole figures are a graphical representation of a texture as variation in diffracted intensity with respect to a direction in the specimen. It can be directly measured with a texture goniometer using X-rays.

Miller indices are a convenient way to represent a direction where directions [u v w] are equivalent to planes (h k l) as we can see in Figure 3.3. The commonest method for specifying a texture component is the plane direction in a crystal. Pole figures are used to derive the Orientation Distribution Function.

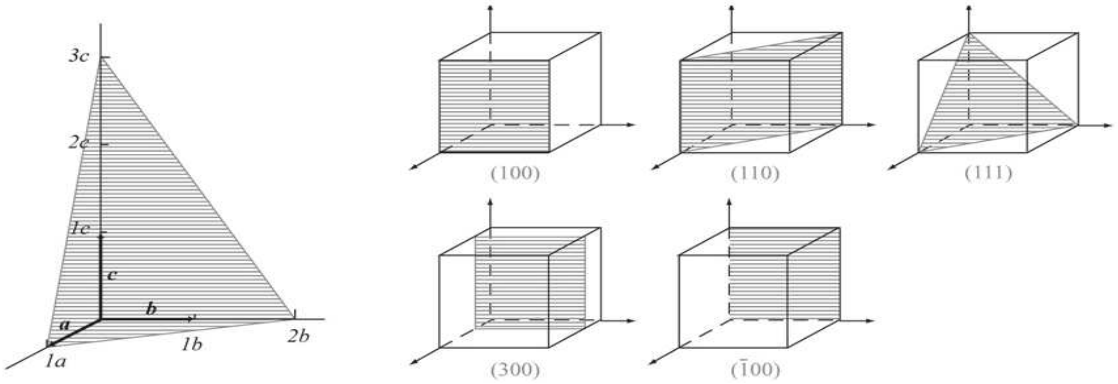

Figure 3.3 Plane designations by Miller indices

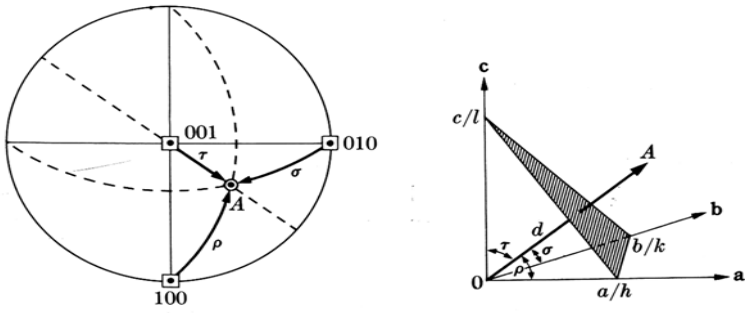

Figure 3.4 Determination of the Miller indices of a pole

If the goniometer is set for a {100} reflection for example, then all the directions in the sample that are parallel to <100> directions will exhibit diffraction as shown in Figure 3.5.

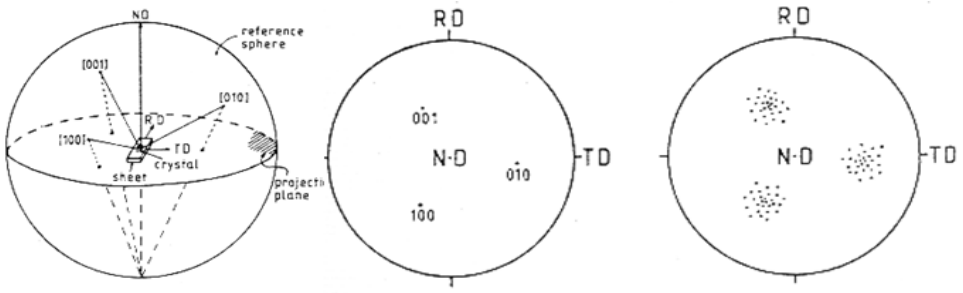

Figure 3.5 Pole figure example

Figure 3.6 shows the experimental and theoretical representation of the texture after the rolling process in the plate by means of 110 pole figure studied in the Department of Metallurgy and Materials Engineering of the Katholieke Universiteit Leuven with thickness

redaction from 1 mm to 0.5 mm. The pole figure of figure 3.6(a) was obtained using a Visco Plsastic Self Consistent model VPSC7b model according to the flow line shown in Figure 3.6(c). As we can see the results are in a good agreement with the available experimental data.

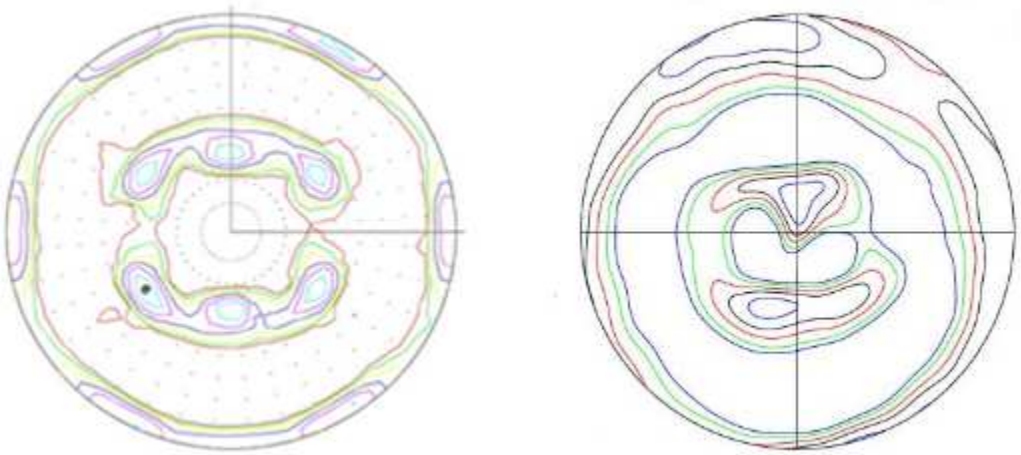

(a) (b)

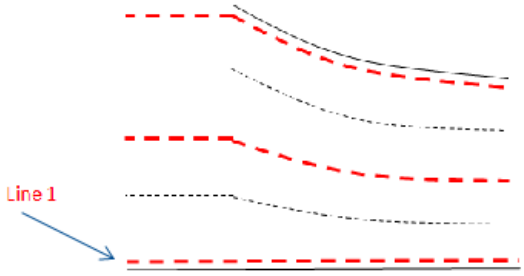

(c)

Figure 3.6(a) theoretical 110 DC04 pole figure. (b) Experimental 110 DC04 pole figure. (c) Flow lines showing that the pole figure was calculated and measured at mid thickness of a rolled plate.

4 RESIDUAL STRESS

4.1 INTRODUCTION

Residual stresses are usually defined as that stress that is internal or locked into a part or assembly even though the part or assembly is free from external forces or thermal gradients.

The main problems associated with rolled steels are related to the surface. During the machining processes the workpiece surface is affected plastically, thermally and chemically. The normal and the friction forces applied by the tool on the workpiece surface generate plastic deformation, resulting in residual stresses in the superficial layer. The formation and propagation of cracks can be initialized by these stresses.

In general, the effects of residual stress can be beneficial or harmful, depending on the magnitude, direction, and distribution of these stresses with respect to the stresses induced by external loads. In general, residual stresses are harmful, and often the predominant factor contributing to fatigue and other structural failure when the tensions in service are added to the residual stresses already present. A particularly insidious aspect of residual stress is that their presence is not detected until failure of the affected component.

It is often important to consider residual stress in failure analysis and design, although residual stress tends to be difficult to visualize, measure and calculate. Residual stress is three-dimensional, self-balanced systems that need not be harmful. In fact, it may be desirable to have high compressive residual stress at the surface of parts subject to fatigue or stress corrosion. The role of residual stress is, therefore, very important when designing mechanical parts.

4.2 STRESS STRAIN BEHAVIOUR

The normal stress across the faces of a block are denoted by σ_x, σ_y and σ_z, where the subscripts denote the directions of the material to the faces. The shear stress acting on the faces normal to the *X* axis is resolved into the components τ_{xy} and τ_{xz} parallel to the *Y* and *Z* axes respectively. The first suffix denotes the direction of the normal to the face and the second suffix the direction of the component. In a similar way, the shear stresses on the face normal to *Y* axis are denoted by τ_{yx} and τ_{yz} and those on the faces normal to the *Z* axis by τ_{zx} and τ_{zy}.The stresses are taken as positive if they are directed as shown in the figure 4.1, when the outward normals to the faces are in the positive directions of the coordinate axes.

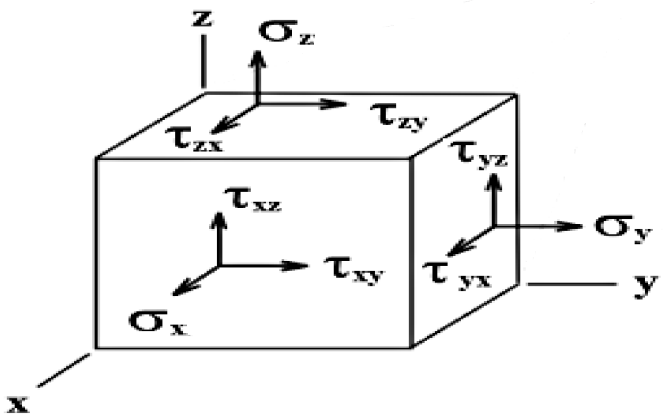

Figure 4.1 Stress directions

The positive directions are all reserved on the remaining faces of the block where the outward normals are in the negative directions of the axes of reference. The nine components of the stress at any point form a second-order tensor σ_{ij}, known as the stress tensor, where *i* and *j* take integral values 1, 2 and 3.The stress components may be displayed as elements of the square matrix.

$$\begin{bmatrix} \sigma_x & \tau_{xy} & \tau_{xz} \\ \tau_{yz} & \sigma_y & \tau_{yz} \\ \tau_{zx} & \tau_{zy} & \sigma_z \end{bmatrix} = \begin{bmatrix} \sigma_{11} & \sigma_{12} & \sigma_{13} \\ \sigma_{21} & \sigma_{22} & \sigma_{23} \\ \sigma_{31} & \sigma_{32} & \sigma_{33} \end{bmatrix} \tag{4.1}$$

Figure 4.2 shows the true stress-strain curve of a typical material in simple tension. So long as the stress is sufficiently small, the material behaves elastically, and the original size of the specimen is regained on removal of the applied load .The initial part of the stress-strain curve is a straight line of slope, which is known as Young´s modulus. The point A represents the proportional at which the linear relationship between the stress and the stress ceases to hold. The elastic range generally extends slightly beyond the proportional limit. For most material, the transition from elastic to plastic behaviour is gradual, owing to successive yielding of the individual crystal grains. The location of the yield point B is, therefore, largely a matter of convention. The corresponding stress Y, known as the yield stress.

Beyond the yield point, the stress continually increases with further plastic strain, while the slope of the stress-strain curve, representing the rate of strain-hardening, steadily decreases with increasing stress.

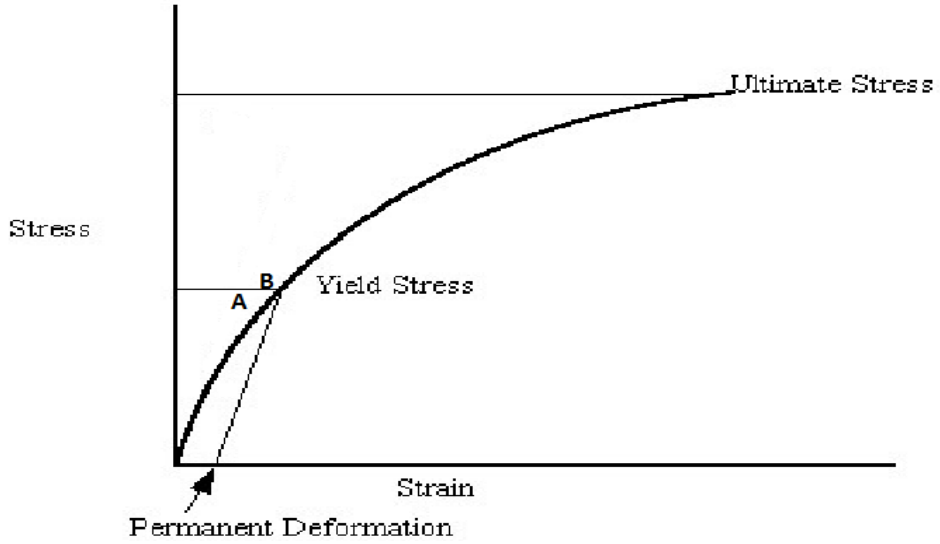

Figure 4.2 Strain-Stress curve.

4.3 MEASUREMENT OF RESIDUAL STRESS

When a metal is being plastically deformed, internal stresses frequently are created due primarily to deformation incompatibilities There have been many methods and techniques proposed for the measurement of residual stress, but only a few may be applied in practice. These few include X-ray diffraction and blind hole drilling with electrical resistance strain gages. A number of procedures have been applied to determine the residual stress extant in a metallic component, as a result of manufacturing processing. However, stress is never the quantity measured because stress is a quantity that is applied to a metal and can only be measured in the process of its application. What is invariably measured to determine residual stress is elastic strain.

X-ray diffraction techniques exploit the fact that when a metal is under stress, the resulting elastic strains cause the atomic planes in the metallic crystal structure to change their spacing. X-ray diffraction can directly measure this interplanar atomic spacing; from this quantity, the total stress on the metal can then be obtained. X-ray can actually measure the interatomic spacings that are indicative of the elastic strain in the specimen. Stress values are obtained from these elastic strain in the crystals by knowing the elastic constant of the material and assuming that stress is proportional to strain as will be explained later.

4.3.1 X-RAY DIFFRACTION

The measurement of deformations by X-ray diffraction is based on Bragg's Law. X-rays are a type of electromagnetic radiation with a high energy and very short wavelengths, practically as the atomic spacing of the solids. When an X-ray beam incident on a solid, a portion of this beam will be scattered in all directions by electrons associated with each atom or ion which is within the beam path. When the parallel X-ray strike a pair of parallel lattice planes, every atom within the planes acts as a scattering centre and emits a secondary wave. All of the secondary waves combine to form a reflected wave. The same occurs on the parallel lattice planes for only very little of the X-ray wave is absorbed within the lattice plane distance, *d*. All these reflected waves interfere with each other. For a defined wavelength and a defined lattice plane distance, this is only given with a specific angle, the Bragg angle θ.

Figure 4.3 shows two planes of atoms which are separated by an interplanar distance *d*. Assuming that an X-ray beam of wavelength λ, parallel, monochromatic and coherent (in phase) impinges on these two planes with an angle ϑ, two rays of this beam (1 and 2), are scattered by the atoms P and Q.

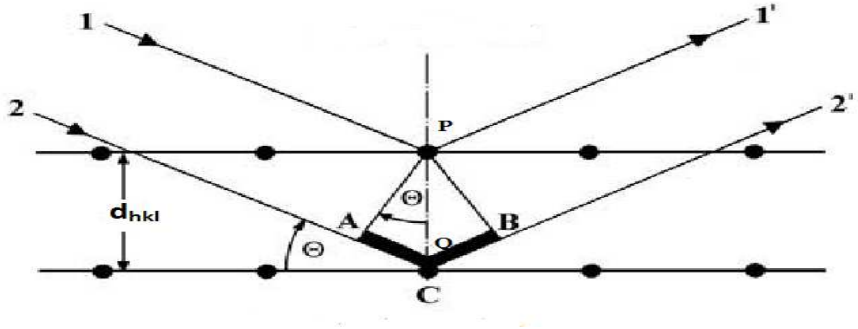

Figure 4.3 Bragg´s law

The proportion of the beam that is scattered on the second plane has a phase difference of 'ABC' to the proportion of the beam that was scattered at the first plane. Following the definition of sine and taking into account that the phase difference is twice:

$$'ABC' = 2d\sin\theta \tag{4.2}$$

When the phase difference is a whole multiple of the wavelength λ:

$$'ABC' = n\lambda \tag{4.3}$$

The equation of Bragg gives the angle of reflection θ of an incoming beam of wavelength λ on a *hkl* plane and the reflected beam (W. Bragg 1912):

$$\lambda = 2d_{hkl}\sin\theta \tag{4.4}$$

What it says is that if we know the wavelength λ of the X-rays going in to the crystal we can measure the angle θ of the diffracted X-rays coming out of the crystal, then we know the spacing between the atomic planes $d_{hkl.}$

4.3.2 OBTAINING STRESSES FROM STRAINS

If one knows the stress-free lattice spacing *hkl d* 0, of the <*hkl*> planes one can calculate the lattice strain:

$$\varepsilon^{hkl} = \frac{d_{hkl} - d_{0,hkl}}{d_{0,hkl}} \tag{4.5}$$

Stresses out of elastic strains cannot be calculated by a single strain measurement because the stress-strain relationship described by a fourth rank tensor by means of the generalized Hook law (J.Nye 1985).

$$\sigma_{ij} = C_{ijkl}\varepsilon_{kl} \tag{4.6}$$

5 CRYSTAL PLASTICITY MODELS

5.1 THEORY OF PLASCITY

The theory of plasticity is the branch of mechanics that deals with the calculation of stress and strain in a body, made of ductile material, permanently deformed by a set of applied forces. The theory is based on certain experimental observations on the macroscopic behavior of metals in uniform states of combined stress. The observed results are then idealized into a mathematical formulation to describe the behavior of metals under complex stresses. Unlike elastic solid, in which the state of strain depends only on the final state of stress, the deformation that occurs in a plastic solid is determined by the complete history of the loading. The microscopic viewpoint deals with a physical explanation of plasticity and established

relationship between plastic behaviour and the interatomic forces acting within the crystal structure of a metal.

Elastic deformation is usually defined as a change in dimensions directly proportional to and on phase with an increase or decrease in applied force. In elastic deformation a limited distortion of the crystal lattice occurs, and as soon as the force is removed, the distortion disappears.

Plastic deformation is commonly defined as a change in dimensions that does or will remain permanent after removal of the load that caused it. In plastic deformation an extensive rearrangement of atoms within the lattice structure takes place resulting in this permanent distortion.

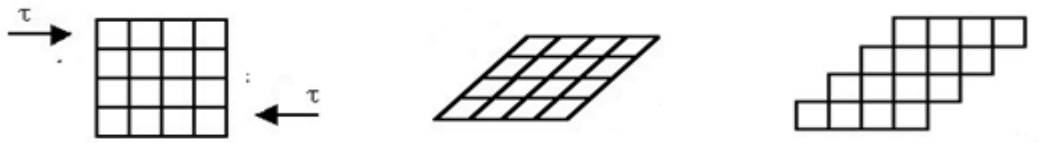

(a) (b) (c)

Figure 5.1: elastic and plastic deformation: sample before stressing (a), elastic (b), plastic(c)

As a result of plastic deformation, the crystallographic directions gradually rotate toward a common axis, producing a preferred orientation. An initially isotropic material thereby becomes anisotropic, and its mechanical properties vary with direction. (J.Chakrabarty 2006).

5.2 SINGLE CRYSTAL PLASTIC BEHAVIOR

The plastic deformation in a grain of a cubic crystal is generally produced by dislocation glide on certain crystal slip systems (UF. Kocks, 1998) , which is the sliding of adjacent blocks of the crystal along definite crystallographic planes called slip planes. The boundary line separating the slipped region of a crystal from the neighboring unslipped region is called a dislocation. The movement of the dislocation, which is responsible for the slip, is initiated by a line defect causing a local concentration of stress. Slip usually occurs on those planes which are most densely packed with atoms.

In body centered cubic (bcc) crystals, like DC04 steel. As shown in Figure 5.2, these slip systems are the <111>slip systems on the {112}, the {110}, and the {123}-plane, although the last systems is only reported by some authors (UF. Kocks, 1998). In this research, the {123}<111>

slip system is not considered. Taken into account the cubic crystal symmetry, there are 24 slip systems.

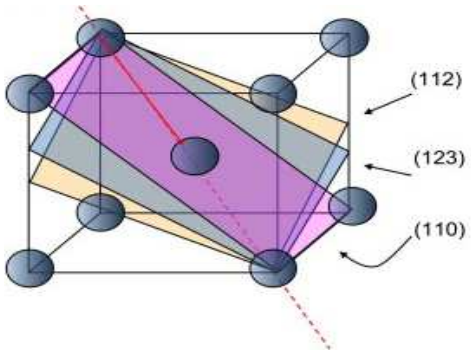

Figure 5.2: <111>slip systems on the (112), (110), (123)-plane in a bcc crystal

The projection of the applied stress on the shear direction in the glide plane is called the *resolved shear stress* on that slip system. Activation of a slip system or plastic deformation, occurs when the "critical resolved shear stress" (CRSS) τ_s on that slip system is reached. This is called the "Schmid law" (UF. Kocks, 1998). It is clear that such as single crystal elasticity, also single crystal plasticity is an *anisotropic* phenomenon.

When the stress is sufficient to permanently deform the metal, it is called plastic deformation which involves the breaking of a limited number of atomic bonds by the movement of dislocations. Thus whenever plastic deformation occurs, and slip occurs on certain slip systems, the crystals rotate in order to maintain compatibility with their surrounding, and finally obtain a non-random orientation distribution. This is schematically shown for a single crystal under tensile load in Figure 5.3. This explains that after severe plastic deformation, the deformed material is always textured (B. Verlinden, 2007).

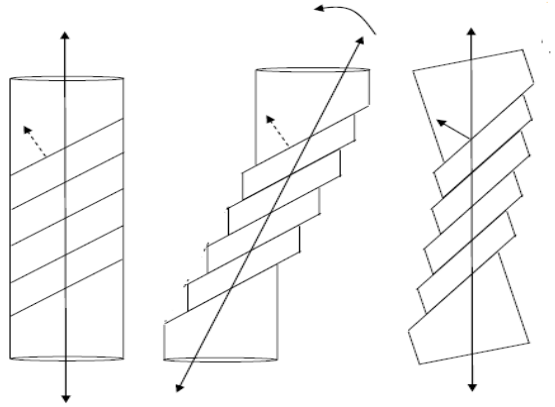

Figure 5.3 monocrystal under uniaxial tensile stress showing plastic deformation by slip and crystal rotation.

5.3 POLICRYSTAL PLASTIC BEHAVIOR

To predict the plastic behavior of a polycrystalline material, several models exist. They can basically be divided into 2 types the Crystal Plasticity Finite Element Models (CPFEM) (L. Delannay, 2006), and crystal plasticity models. In the first method, a set of several grains (typically 1000) is divided in finite elements, where one grain consists at least of one element. The method requires several orders of magnitude of the calculation time of a crystal plasticity model (Van Houtte P. S., 2005), and is therefore not suitable for online use. From now on only the latter models are considered.

In crystal plasticity models, the macroscopic velocity gradient (or accumulated: the deformation gradient) tensor is imposed, whereas the stresses and strains in the grains, as well as the macroscopic stress, are obtained supporting on specific assumptions. Some important models are the Taylor model (Taylor, 1938), the visco-plastic self consistent model (R.A. Lebensohn, 1993), the Alamel model (Van Houtte P. S., 2005), and the GIA model (M. Crumbach, 2001). Although having proved their usefulness, the descriptions of plasticity with crystal plasticity models are considered to be extremely simple in comparison to the underlying physical phenomena (CN. Tome, 2007). The first 3 will be explained briefly below. A schematic representation of the assumptions in these 3 models is given in Figure 5.4.

When the same critical resolved shear stress is adopted for all the slip systems, the Taylor factor M is defined as the power per unit of volume divided by a measure for the equivalent strain rate, usually the Von Mises equivalent strain rate, and the CRSS:

$$M = \frac{P}{\dot{\varepsilon}_0 \tau^c} = \frac{\sigma_{eq}}{\tau^c} \tag{5.1}$$

The Taylor factor is only dependent on the strain mode, not on the magnitude of the equivalent strain rate. Since the power per unit of volume is equal to the product of the equivalent strain and the equivalent stress, the Taylor factor equals the equivalent stress, relative to the CRSS (second part of equation) if a scalar isotropic hardening law is assumed, the Taylor factor multiplied by the CRSS can be seen as the isotropic yield stress. This approach is taken in this work.

5.4 TAYLOR MODEL

In a Taylor model, every grain is supposed to have the same strain and strain rate, being equal to the macroscopic strain and strain rate (Taylor, 1938). This means that the Taylor model assumes no grain interaction. Initially, each crystal has an orientation with respect to a sample coordinate system in order to make the ODF of the polycrystal in the model corresponds to the one of the initial texture. As an additional assumption, a minimum in internally dissipated frictional work rate is assumed (Taylor, 1938).

5.5 VISCO-PLASTIC SELF CONSISTENT MODEL

In a self-consistent crystal plasticity model, each grain is considered as a visco-plastic anisotropic ellipsoidal Effective Medium (HEM) (R.A. Lebensohn, 1993). The stress and strain-rate are uniform inside the inclusion, but different from the macroscopic stress and strain rate. The stresses and strains in the grains, as well as the macroscopic stress, are obtained by solving the stress equilibrium equation for the homogeneous medium (CN. Tome 2007). A power law with a strain rate sensitivity describes the relationship between the resolved shear stress and the shear strain rate on a certain slip system (L.S. Toth, 1988). Inclusion embedded in a visco-plastic anisotropic Homogeneous

5.6 ALAMEL MODEL

The Advanced Lamel Model is similar to the Taylor model, but the interaction of each grain with 1 neighbour is taken into account by forbidding grain boundary sliding, and consequently imposing stress equilibrium at the grain boundaries (Van Houtte P. L., 2002) (Van Houtte P. S., 2005). Additional to the orientation distribution function for crystal orientations, more information about the initial microstructure has to be provided by means of a grain boundary segments orientation distribution function (GBSODF). Although the calculation time is of the same order of magnitude as a Taylor model, it is able to predict the deformation textures more accurately (Van Houtte P. S., 2005).

In the Figure 5.4 one can see the schematic representation of the assumptions made in a Taylor model where every grain is supposed to have the same strain rate, Alamel model in which the interaction of each grain with one neighbour is taken into account by forbidding grain boundary sliding and visco-plastic self consistent model where each grain is a visco-

plastic anisotropic ellipsoidal inclusion embedded in a visco-plastic anisotropic Homogeneous Effective Medium.

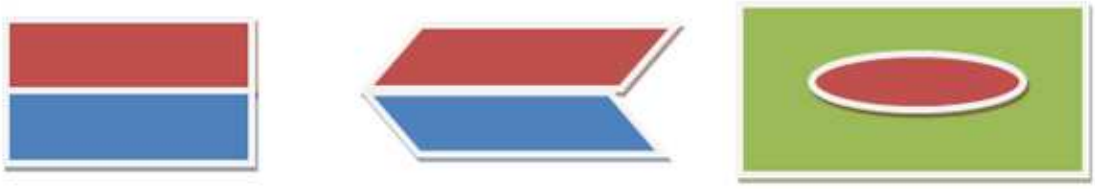

(a) (b) (c)

Figure 5.4 (a) Taylor Model,(b) Alamel Model (c) Visco-Plastic Self Consistent Model

For this chapter has been used as a reference “Koen Decroos , Marc Seefeldt, internal report”

5.7 IMPUT PARAMETERS FOR A CRYSTAL PLASTICITY MODEL

The most important input of the model are the imposed macroscopic velocity gradient tensor, the initial texture and monocrystal data such as grain shape, the slip systems, and strain rate sensitivity. They are only briefly discussed here.

5.7.1 VELOCITY GRADIENT AND DEFORMATION GRADIENT TENSOR

Consider a body B that result in a body B’ after deformation, as seen in Figure 5.5:

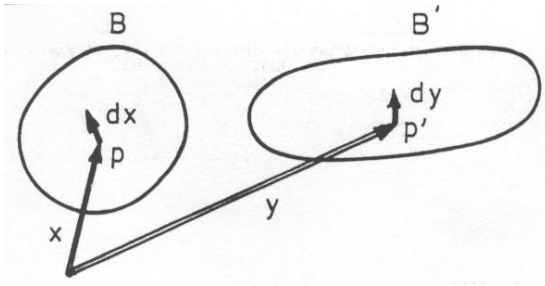

Figure 5.5: definition of coordinate systems of a body B that undergoes a deformation and becomes a body B’

Supposing the function $\underline{y} = \underline{y}(\underline{x}, t)$ describes the deformation of the body B, the velocity gradient tensor is given by equation 5.2, in tensorial form.

$$\underline{\underline{L}} = \frac{\partial \underline{v}}{\partial \underline{y}} \qquad L_{ij} = \frac{\partial v_i}{\partial y_j} \tag{5.2}$$

The deformation gradient tensor is defined by equation 5.3.

$$\underline{\underline{F}} = \frac{\partial \underline{y}}{\partial \underline{x}} \qquad F_{ij} = \frac{\partial y_i}{\partial x_j} \tag{5.3}$$

Following relationship between both tensors exist:

$$\underline{\underline{L}} = \dot{\underline{\underline{F}}}\,\underline{\underline{F}}^{-1} \tag{5.4}$$

5.7.2 INITIAL TEXTURE

The initial texture is usually given by means of a *texture file* which is a text file with a discrete set of grains with orientations $(\varphi_1, \phi, \varphi_2)$ (Bunge, 1982) with respect to a sample reference system, representing the statistical distribution of the texture. After cold rolling, the deformed crystals recrystallise and have weaker texture than before. In this work, it is supposed that the material has a random texture after the cold rolling process.

5.7.3 MONOCRYSTAL DATA

The monocrystal data briefly discussed here are those needed in the Visco Plastic Self consistent model VPSC7b. The most important ones are the grain shape, the slip systems, the strain rate sensitivity, and the single crystal hardening law. In VPSC7b, the single crystal has a work hardening law where the hardening is only depending on the accumulated shear strain in the grain, as seen in formula 5.5. An extended Voce hardening law (Voce, 1948) is used.

$$\tau^s = \tau_0^s + \tau_1^s\left(1 - \exp\left(-\Gamma\left|\frac{\theta_0^s}{\tau_1^s}\right|\right)\right) \tag{5.5}$$

With $\Gamma = \sum_s \Delta\gamma^s$ the accumulated shear in the grain, and τ_0^s, θ_0^s, $\tau_0^s + \tau_1^s$ the initial CRRS, the asymptotic hardening rate and the back-extrapolated CRRS (CN. Tome, 2007).In the current study, the Voce parameters were fitted to reproduce the experimental macroscopic stress-strain curve.

6 COMPUTATIONAL: FAST MATERIAL MODEL FOR ROLLING PROCESSES

6.1 FAST IMPLEMENTATION OF THE MATERIAL LAW PREDICTED BY CRYSTAL PLASTICITY MODELS: DATABASE PRINCIPLE

The most obvious way to calculate the Taylor factor at a certain point in a deformed metal based on a crystal plasticity model is to calculate the deformation gradient tensor, and use that as an input for a crystal plasticity model. In the framework of current project, the best way to generate the deformation gradient tensor is using by the flowline model like explained above. The data flow for 1 grid point is shown in Figure 6.1.

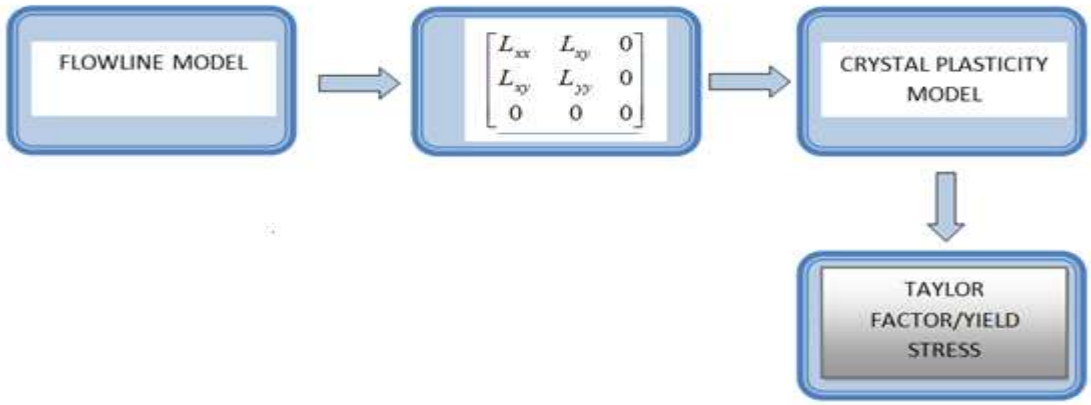

Figure 6.1: The data flow to calculated the Taylor factor for 1 grid point

(ref. Online use of physically based plasticity models for steady state forming processes, K. Decroos, M. Seefeldt, in progress)

The time for generation of a tensor is much less then 1s, whereas the time to run the crystal plasticity model for a set of 1000 grains is approximately 6 seconds on a normal computer. The total calculation time therefore determined by the runtime of a crystal plasticity model, and is way too high if online process control is wanted. Since the calculation time of a crystal plasticity model cannot be reduced drastically without significant loss of accuracy and these calculations have to be made at every grid point in space considered by the layer model, this way of calculating the material behavior is not suited for online process control.

For the purpose of online process control, a new method has been developed that makes the computationally costly calculations offline, before the process starts. A DOS batch file has been written to make the VPSC7b model run for a discrete grid in 2 dimensional tensor space covering all possible deformation modes of a realistic cold rolling process. Per deformation mode, all the information about texture and anisotropy are stored in a database.

Online, for all points in 2 dimensional points in space, the velocity gradient tensor and the deformation gradient tensor are generated based on either a flowline model or the layer model. The choice between both can be specified by the user. Per grid point, the tensor *F* is compared to the tensors *Fj* in the database. The selection of the database tensor *Fi* that is the best estimation for the tensor *F* is the tensor for which criterion 6.1 is fulfilled:

$$\left\| \underline{\underline{F}}_i - \underline{\underline{F}} \right\| = \min_j \left(\left\| \underline{\underline{F}}_j - \underline{\underline{F}} \right\| \right) \tag{6.1}$$

With the norm of a tensor defined is by equation 6.2:

$$\left\| \underline{\underline{F}} \right\| = \sqrt{\sum_{i,j} F_{ij}^2} \tag{6.2}$$

Obviously, the finer the grid in tensor space, the better the estimate the database tensor is for the calculated tensor. The stored Taylor factor can then be queried directly. The principle is shown in Figure 6.2.

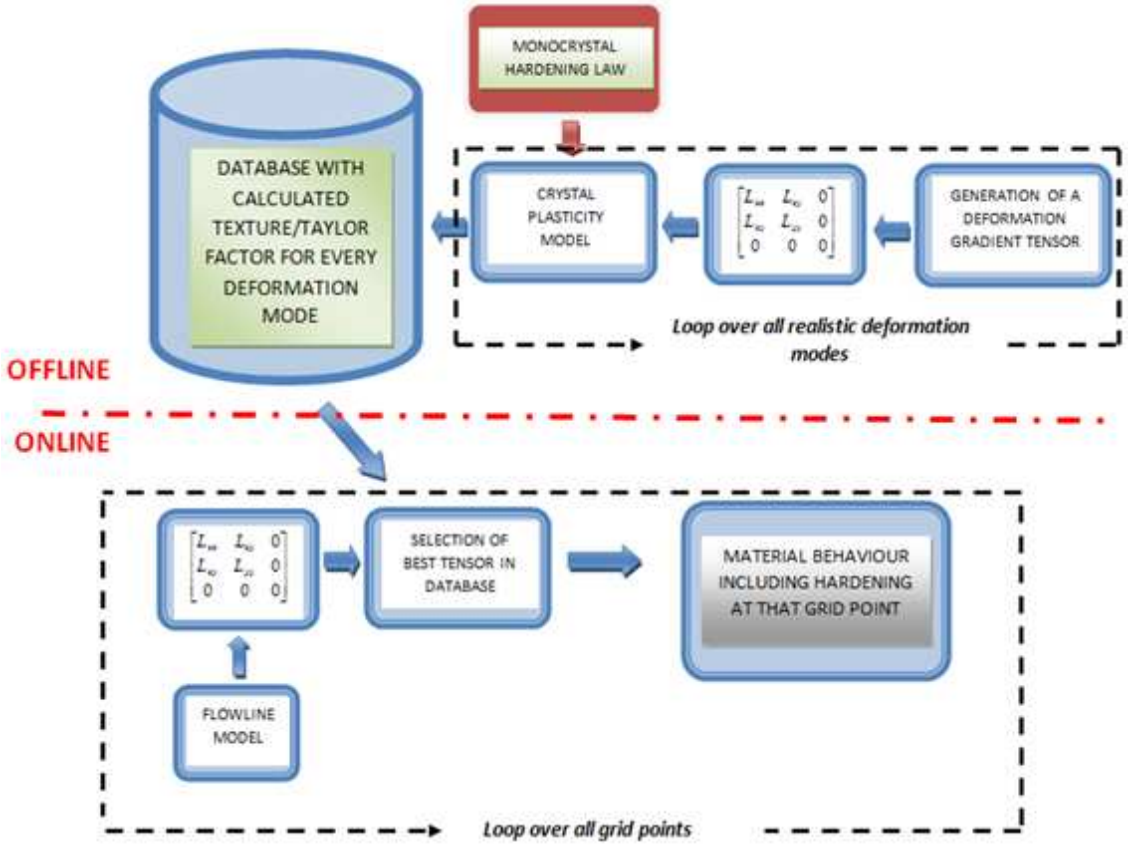

Figure 6.2: Schematic representation of the database principle for material behavior prediction.(ref. Online use of physically based plasticity models for steady state forming processes, K. Decroos, M. Seefeldt, in progress)

In the explained method the material hardening parameters (Voce hardening on the slip systems) are incorporated in the database and cannot be changed online.

The online generation time of a deformation gradient tensor is depending on the models used. When a tensor is given, the selection time of the best suited tensor of the database is 0.0022s for a database consisting of 10000 tensors. It is clear that the total calculation time will increase with an increase of grid points per layer, an increase of number of layers, and an increasing number of deformation modes in the database. On optimal balance between time cost and accuracy should be investigated in the future.

7 RESULTS OF A MATERIAL MODEL WITHOUT SINGLE CRYSTAL HARDENING

The results shown here are results for the Taylor factor, crystallographic texture by means of 110 pole figures (Bunge, 1982), and plastic anisotropy by means of π-plane projections of yield surfaces (U. Kocks, 1998). The results are simulated for single crystals without (Voce) hardening on the slip systems. Consequently, the difference of Taylor factor is only due to texture: texture hardening is shown here.

7.1 TAYLOR FACTOR

The prediction of the Taylor factor at 3 positions is made for 3 crystal plasticity models: Taylor, Alamel, and VPSC7b. the results are shown in Figure 7.1. The Taylor model predicts the highest Taylor factor. Every model shows a difference at the 3 positions. The case studied is for a rolling of a plate with a thickness reduction from 1 mm to 0.7 mm and mill radius of 235 mm.

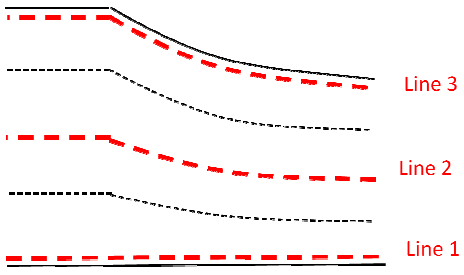

	Taylor	Alamel	VPS7b
Line3	2.742	2.572	2.66
Line 2	2.740	2.551	2.645
Line1	2.714	2.491	2.618

Figure 7.1: Taylor factor at the end of the rolling pass for 3 positions in the plate.

7.2 TEXTURE

Figure 7.2 shows the texture after rolling pass for 3 positions in the plate by means of 110 pole figure with thickness reduction from 1mm to 0.7 mm and rolling mill radius of 235mm.

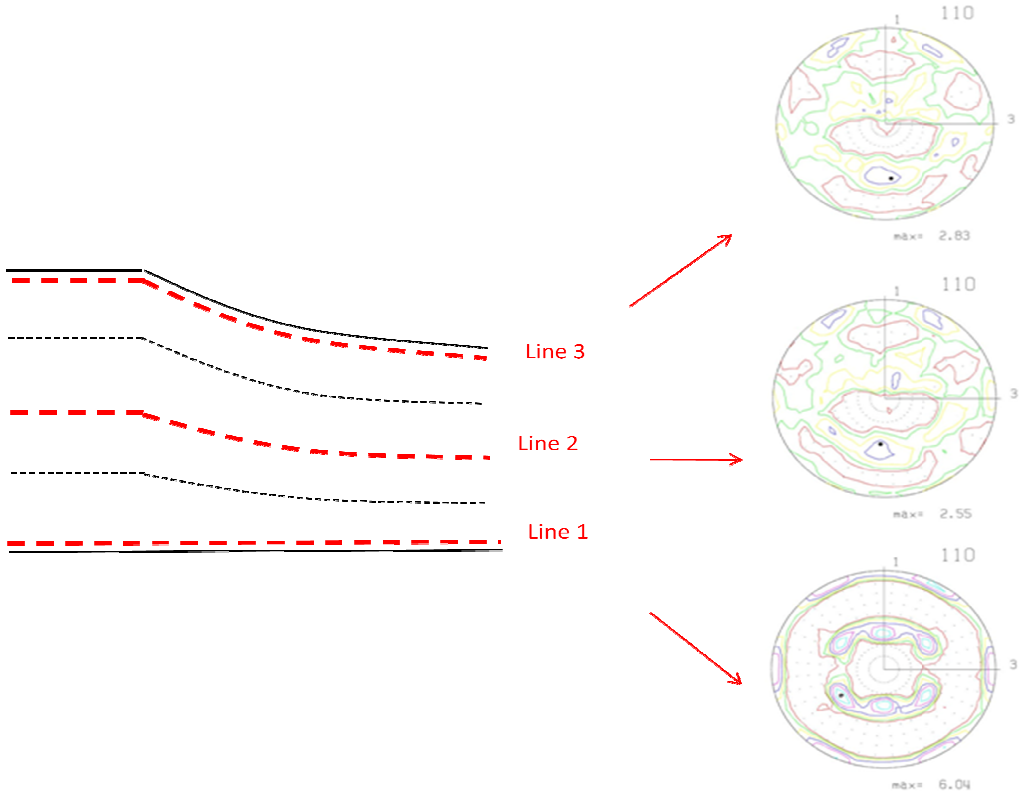

Figure 7.2: Texture after the rolling pass for 3 positions in the plate by means of a 110 pole figure. The texture is predicted by the VPSC7b crystal plasticity model.

7.3 PLASTIC ANISOTROPY

Figure 7.3 shows the π-plane representations of the yield surfaces of the rolling pass for 3 positions in the plate where the yield surfaces are predicted by the VPSC7b crystal plasticity model.

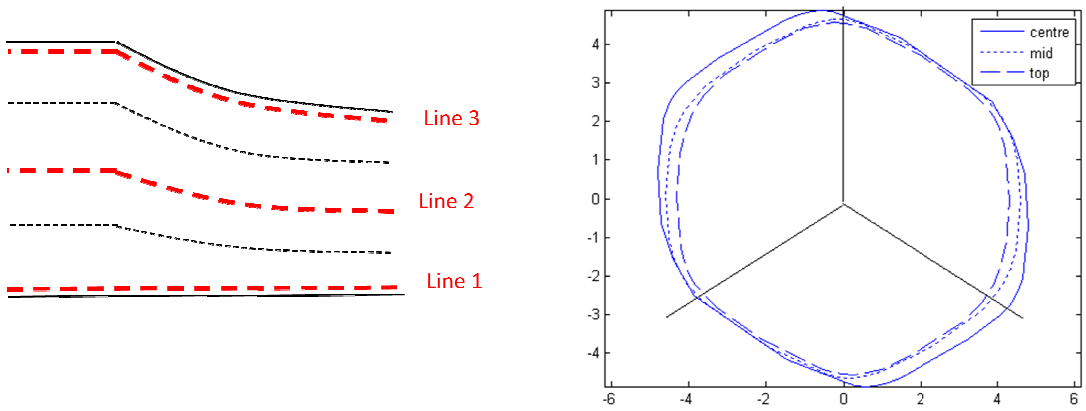

Figure 7.3: π-plane representations of the yield surfaces of the rolling pass for 3 positions in the plate. The yield surfaces are predicted by the VPSC7b crystal plasticity model.

8 CALIBRATION OF THE SINGLE CRYSTAL PARAMETERS

Known the texture and anisotropy simulated without single crystal hardening, the aim of this work is to find the single crystal plastic parameters described by the Voce hardening law so that incorporate it in the database used as an imput in a polycrystal plasticity model, in our case VPSC, to calculate more accurate representation of the evolution of texture, anisotropy and hardening in any kind of deformation process.

In order to predict the plastic behavior of a polycrystalline material, VPSC crystal plasticity model allows us to obtain the stress and strain in the grains as well as the macroscopic stress once the macroscopic velocity gradient tensor, initial texture and monocrystal data are imposed as imputs.

8.1 SINGLE CRYSTAL BEHAVIOUR

Given that the plastic response on the grain level is described by the Voce hardening law, an extended Voce law (Figure 8.1) is used in visco-plastic self consistent model to describe the hardening of a slip system, thus in the current study, the Voce parameters were fitted to reproduce the experimental stress-strain curve simulating.

$$\tau^s = \tau_0^s + \tau_1^s(1-\exp(-\Gamma\left|\frac{\theta_0^s}{\tau_1^s}\right|)) \qquad (8.1)$$

Where $\Gamma = \sum_s \Delta\gamma^s$ the accumulated shear in the grain, and τ_0^s, θ_0^s, $\tau_0^s + \tau_1^s$ the initial CRRS, the asymptotic hardening rate and the back-extrapolated CRRS (CN. Tome, 2007).

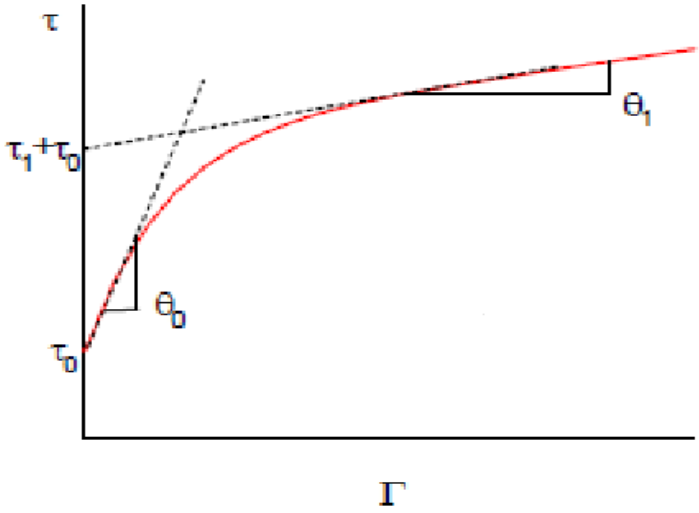

Figure 8.1. Extended Voce law used in VPSC to describe the hardening of slip and twin systems vs accumulated shear in grain Γ.

During plastic deformation, the metal atoms are permanently displaced from their original positions and take up new positions. The ability of some metals to be extensively plastically deformed without fracture under the action of a shear stress is one of the most useful engineering properties of metals.

Hardness is a measure of the resistance of a metal to permanent or plastic deformation. Thus the hardness of a metal depends on the case with which it plastically deforms. Thus the relationship between hardness and strength for a particular metal can be determined making use of the tensile test.

Work hardening is a consequence of the fact that the stress required for dislocation movement usually increases during plastic flow as the dislocations become increasingly hindered by microstructural obstacles. The interaction of moving dislocations with other dislocations normally constitutes a barrier to further movements which requires an increase in the stress flow for the dislocations to keep moving. Work hardening influence the amount of energy stored in the material as a consequence of plastic deformation.

Dislocation produce atomic displacements on specific crystallographic slip planes and in specific crystallographic slip directions. The slip planes are usually the most densely packed planes, which are also the farthest separated. The stress required to cause slip in a pure-metal single crystal depends mainly on the crystal structure of the metal, its atomic bording characteristic, the temperature at which it is deformed, and the orientation of the active slip planes with respect to the shear stress. Slip begins within the crystal when the shear stress on the slip plane in the slip direction reaches a required level called the critical resolved shear stress. Essentially, this value is the yield stress of a single crystal and is equivalent to the yield stress of a polycrystalline metal or alloy determined by a stress-strain tensile test curve.

The solution of such an inverse problem has to be found by searching these single crystal parameters that give the best agreement with certain experimental data. The best agreement is expressed by minimizing a cost function Y, here given by the summation of the squares of the differences between observed values and modeled output values.In this research, these values are equivalent stresses and strains from a tensile test. Each measured stress-strain point i is a point to consider in the cost function of equation 8.1.

$$Y = \sum_{i} (\sigma_{i,EXP} - \sigma_{i,MODEL})^2 \tag{8.1}$$

The experimental equivalent stress $\sigma_{i,EXP}$ is the one corresponding to the jth point of the jth mechanical test. The modeled equivalent stress $\sigma_{i,MODEL}$ correspond to the calculated equivalent stress for the accumulated deformation in point j of test i, based on a crystal plasticity model. This work supports a simplex algorithm, which is a direct search algorithm (Murty 1983), in that sense that initial values for the algorithm are investigated by manually minimizing the cost function of equation 8.1, and that the sensitivity of these parameters has been investigated.

The strain rate sensitivity *n* is used in the viscoplastic law on each activated slip system giving the relationship between stress and strain rate per slip system:

$$\frac{\dot{\gamma}}{\dot{\gamma}_0} = \left(\frac{\tau^s}{\tau_0} \right)^n \tag{8.3}$$

The aim of current research is to find the optimal values for the parameters τ_0, τ_1, θ_0 and n, for a DC04 and a DC01 steel, based on tensile test made in the laboratory. The stress-strain curve is shown in Figure 8.2.

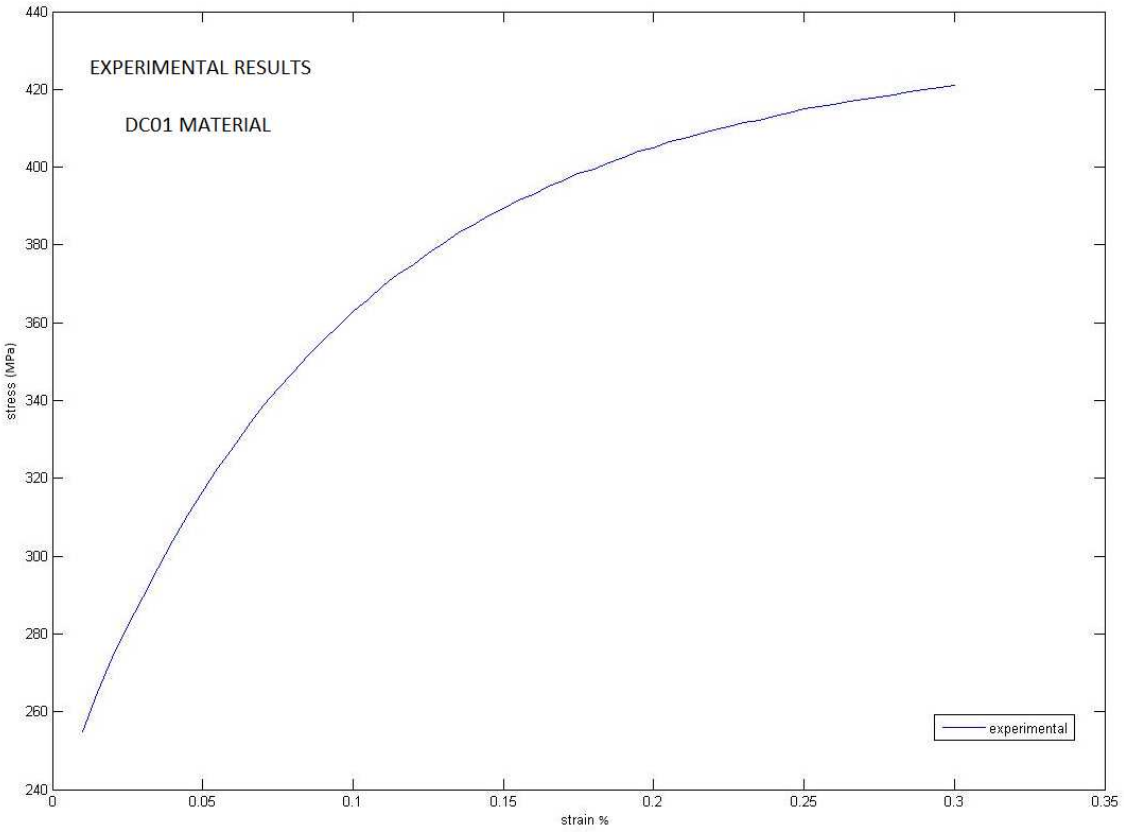

(a)

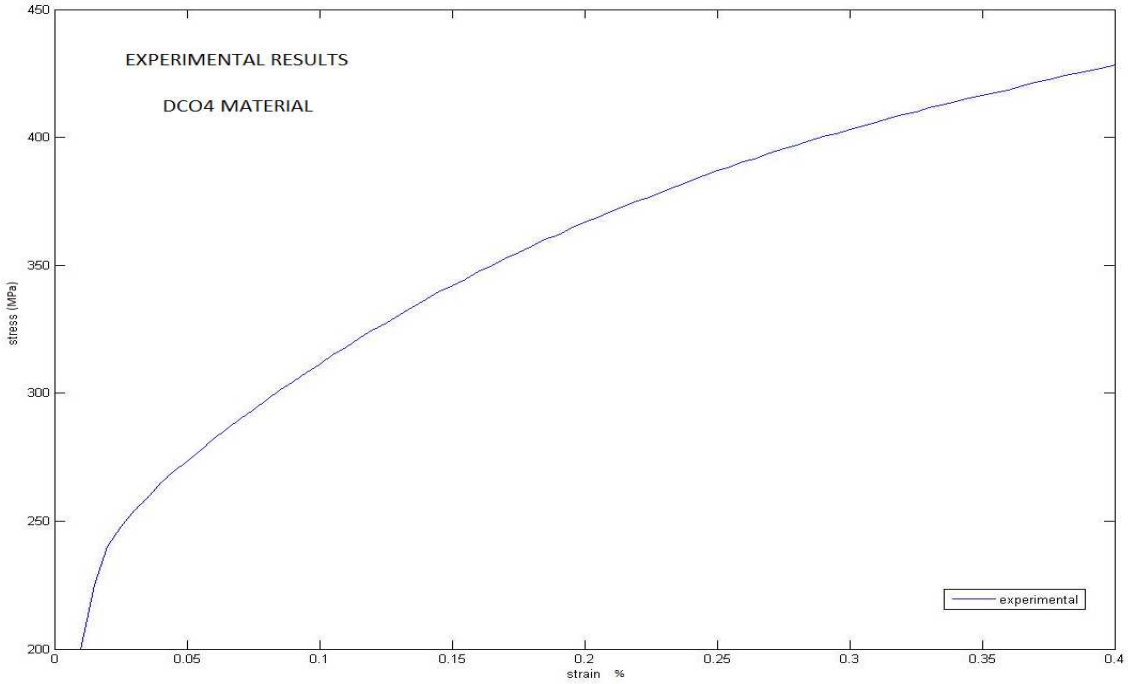

(b)

Figure 8.2. (a) Experimental DC01 stress-strain curve.(b) Experimental DC04 stress-strain curve.

Thus in the present work will be simulated 59 points in DCO1 case and 79 points in DCO4 in order to find the best agreement between the points represented using VPSC model for different values of Voce single crystal parameters and the given macroscopic stress-strain experimental curve.

The values found by the manual fit for the different parameters are shown in table 8.1:

DCO1			
$\tau_0 = 101MPa$	$\tau_1 = 79\,MPa$	$\theta_0 = 385MPa$	$N = 25$
DC04			
$\tau_0 = 102MPa$	$\tau_1 = 102\,MPa$	$\theta_0 = 200MPa$	$N = 20$

Table 8.1 Parameters values

The resulting predicted stress-strain curves based on these parameters shown above (broken line), together with the experimental ones given (unbroken line), are shown in Figure 8.3.

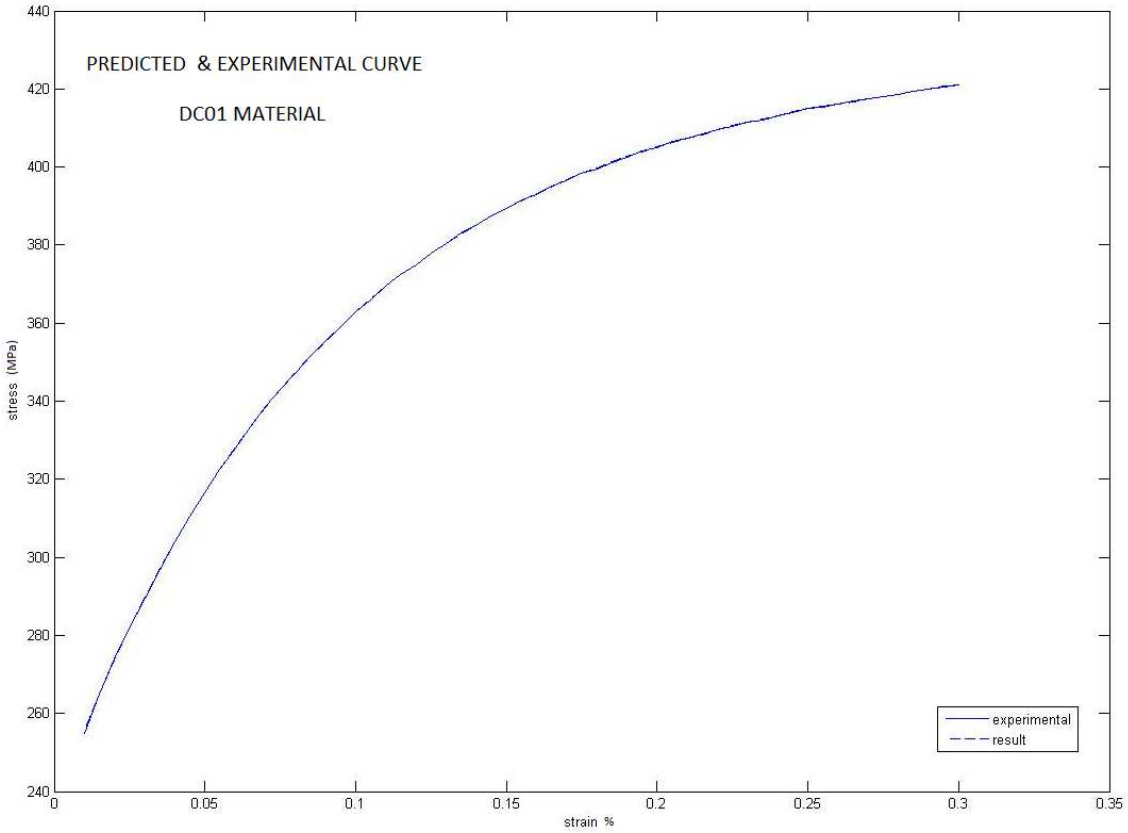

(a)

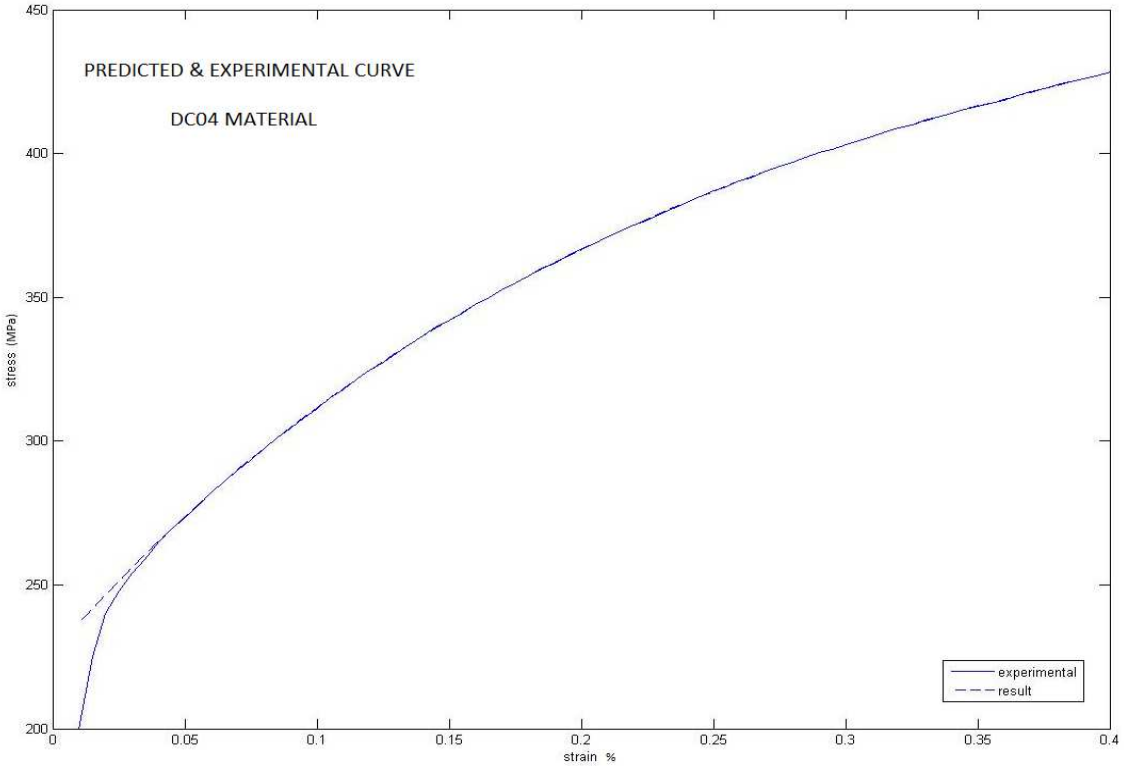

(b)

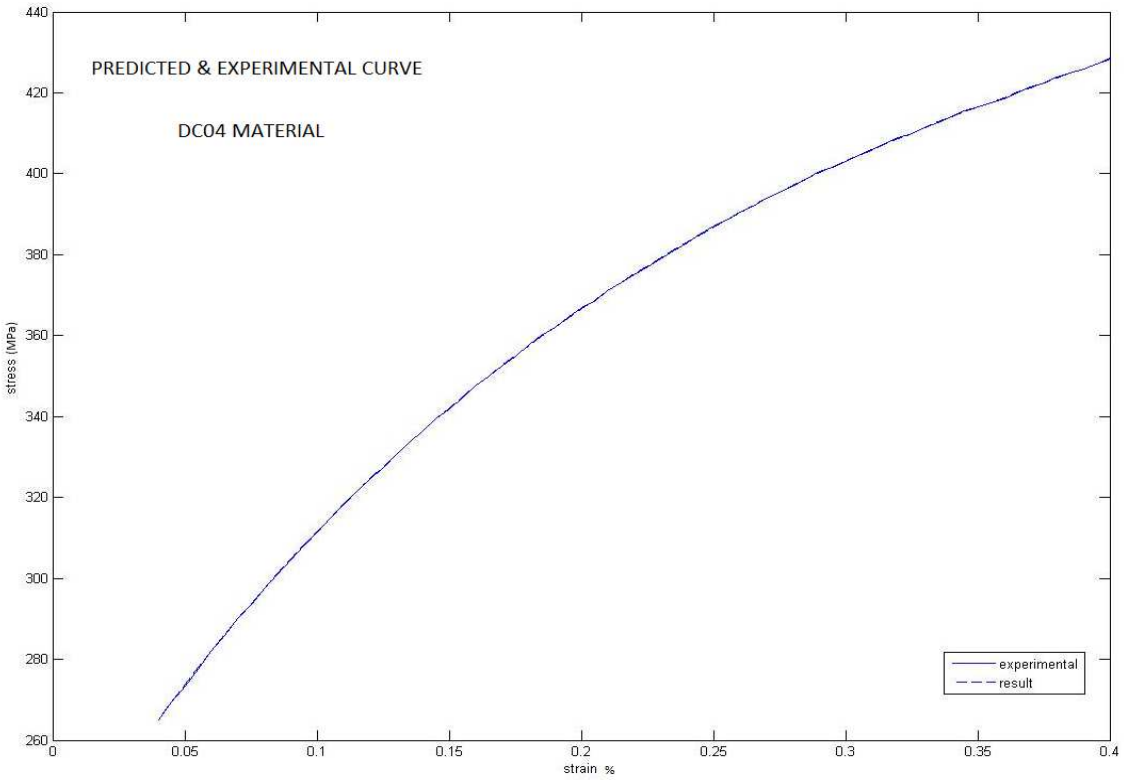

(c)

Figure 8.3(a) Result stress-strain curve. (a) DC01, (b) DC04, (c) values from 0, 04 on in DC04.

As can be seen in figure 8.3(b) the lowest values do not fit the experimental curve in DC04 case. We are using figure 8.2(c) to see clearer how it fit from 0,04 on.

Once we found the fitter parameters we are able to study the influence of each one.

8.2 CRITICAL RESOLVED SHEAR STRESS

The initial critical resolved shear stress parameter τ_0 indicates the value at which the activation of a slip system or plastic deformation within the crystal occurs. Thereby, when τ_0 is reached, the crystal will start to yield and the dislocations will start to move throughout the most favorably oriented slip system. Thus, in our case we can see the differences appeared in the macroscopic stress-strain curve under the influence of several critical resolved shear stress values. An increase in τ_0 of 5 MPa, shown in the green curve, in regard to the value fitted (blue curve),is equivalent to an increase of 12 MPa on the macroscopic stress values and in the same way a decrease of 5 MPa, shown in the red curve, is equivalent to a decrease of 12 MPa in the macroscopic stress value (Figure 8.4).It describe how τ_0 influences in the increment or decrement of the stress needed to maintain the plastic deformation along the material.

As the critical resolved shear stress value increases, can be seen that both the stress required for elastic and plastic deformation increases as well as the yield strength.

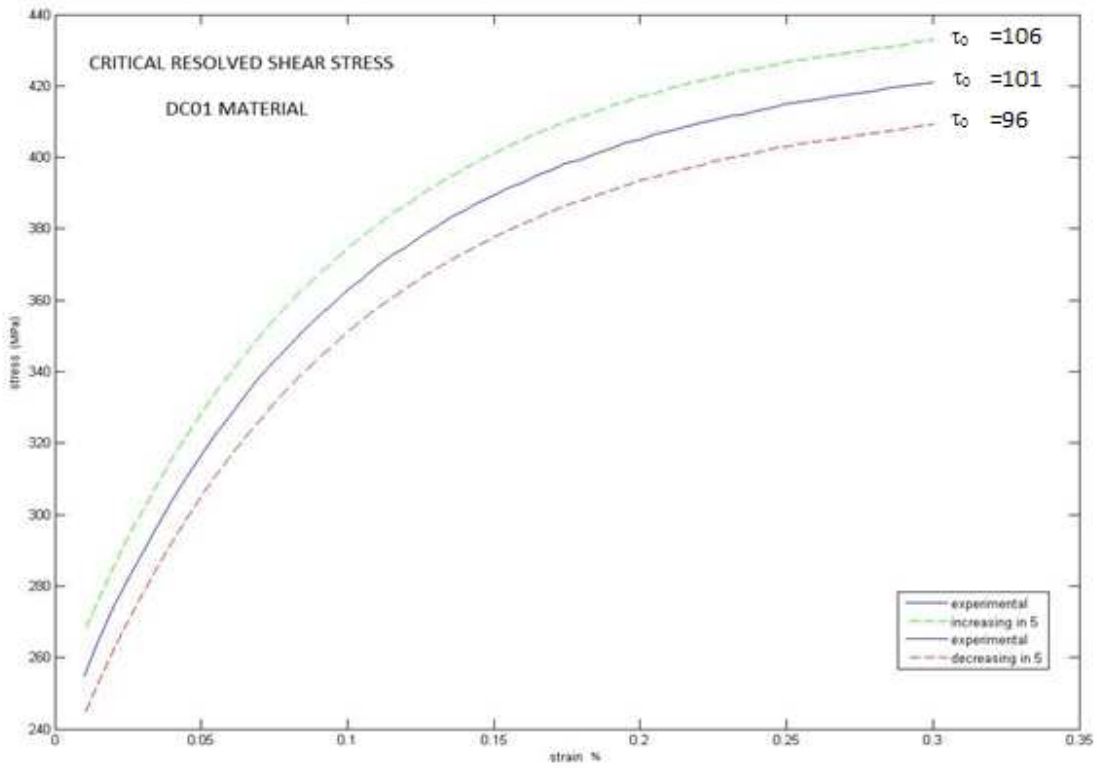

(a)

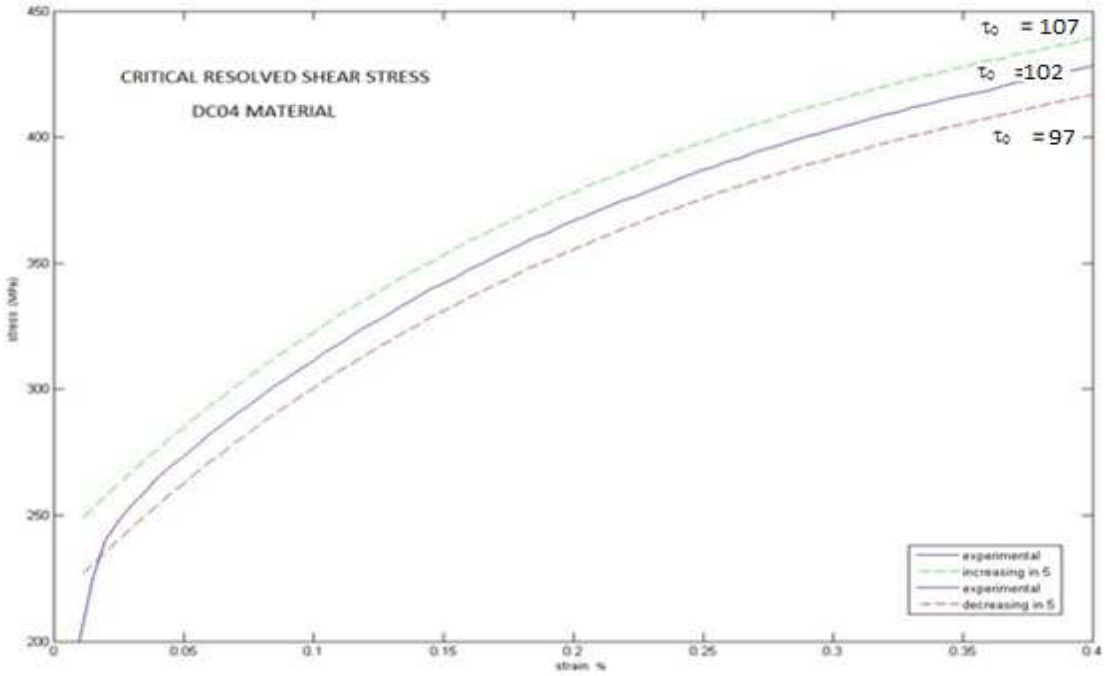

(b)

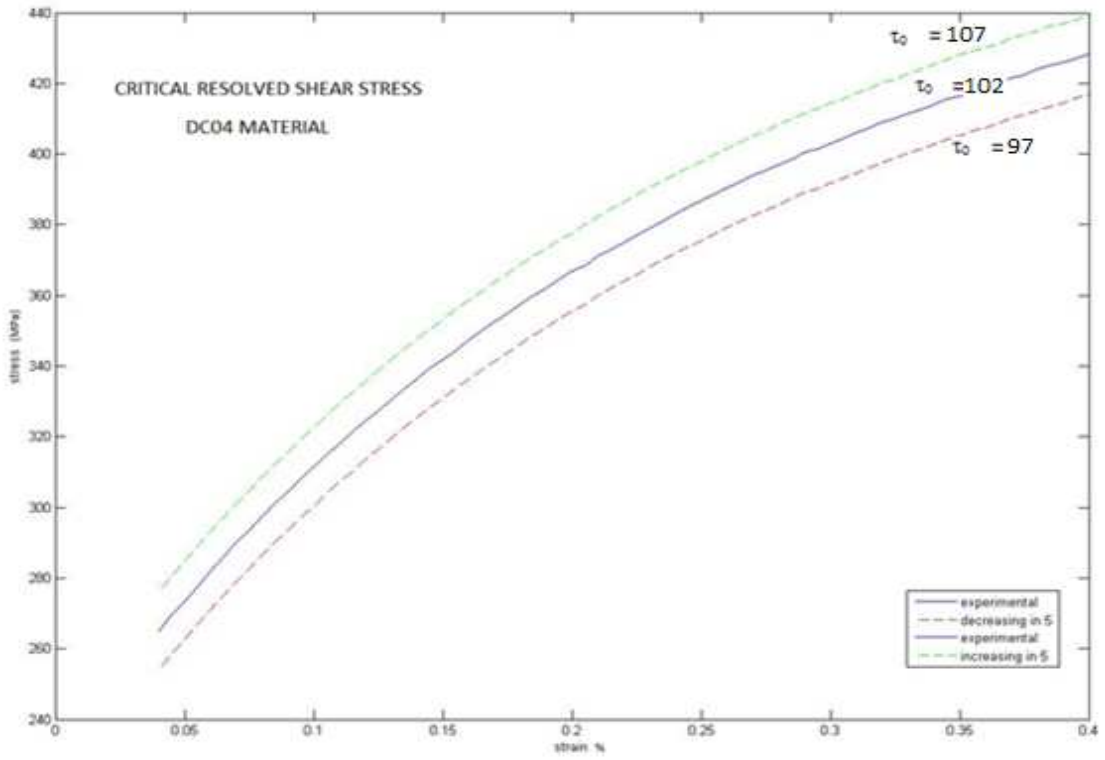

(c)

Figure 8.4 stress-strain curves for different τ_0 values. (a) DC01, (b) and (c) DC04.

8.3 STRAIN RATE SENSITIVITY

The strain rate sensitivity parameter *n* refers to the response of a material´s flow stress and hardening rate to changes in strain rate or deformation behavior. Hence *n* is a measure of the rate sensitivity of the hardening rate as it affects the shape of the curve and allows a gradually increase in the initial and final stress values although the increment of the final value is greater due to a higher initial slope (Figure 8.5).

The increase in the rate sensivility is of main relevance since it is assumed that this rate sensivility acts homogenizing materials behavior, increasing their ductility and delaying plastic localization.

Can be shown in the figure that the yield stress point increases with increasing the strain rate sensitivity.

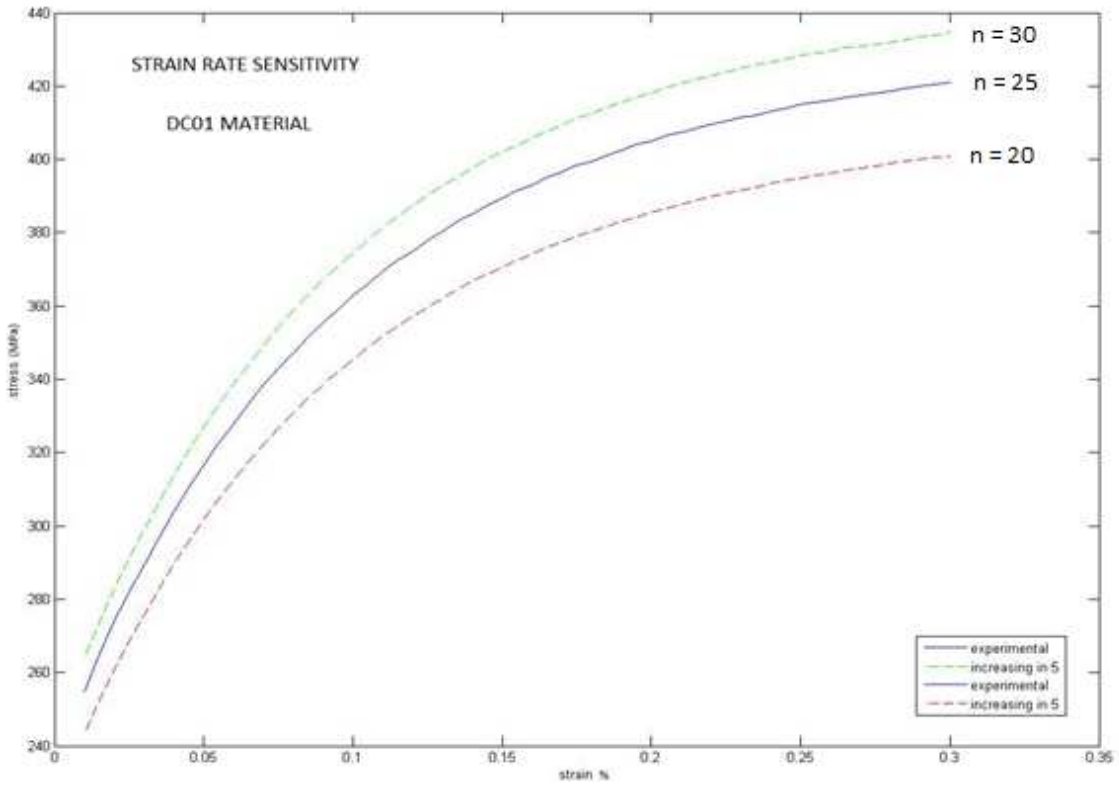

(a)

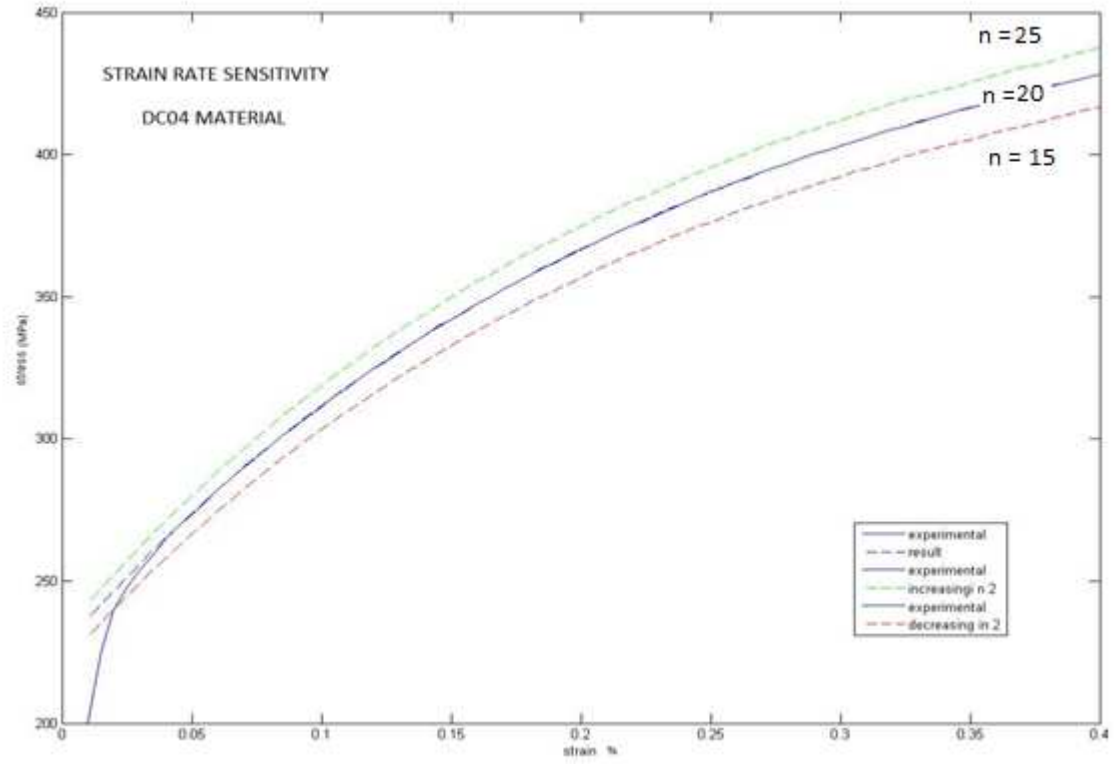

(b)

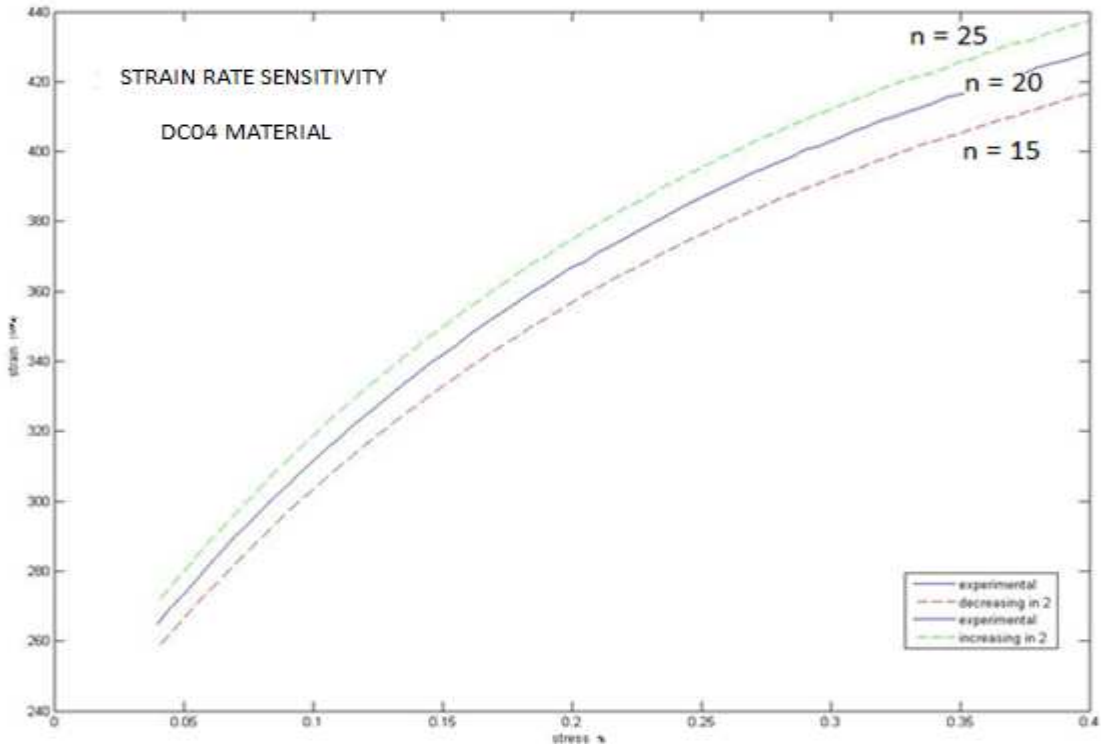

(c)

Figure 8.5 stress-strain curves for different *n* values. (a) DC01, (b) and (c) DC04.

8.4 BACK EXTRAPOLATED CRITICAL RESOLVED SHEAR STRESS

Following an incremental increase in τ_1, an increasing divergence in the slope is noticed. However, it has no influence on the initial stress value and the initial slope (Figure 8.6). It means that this value has not influence in the yield stress, however at some point make necessary to increase the stress required to maintain the plastic deformation.

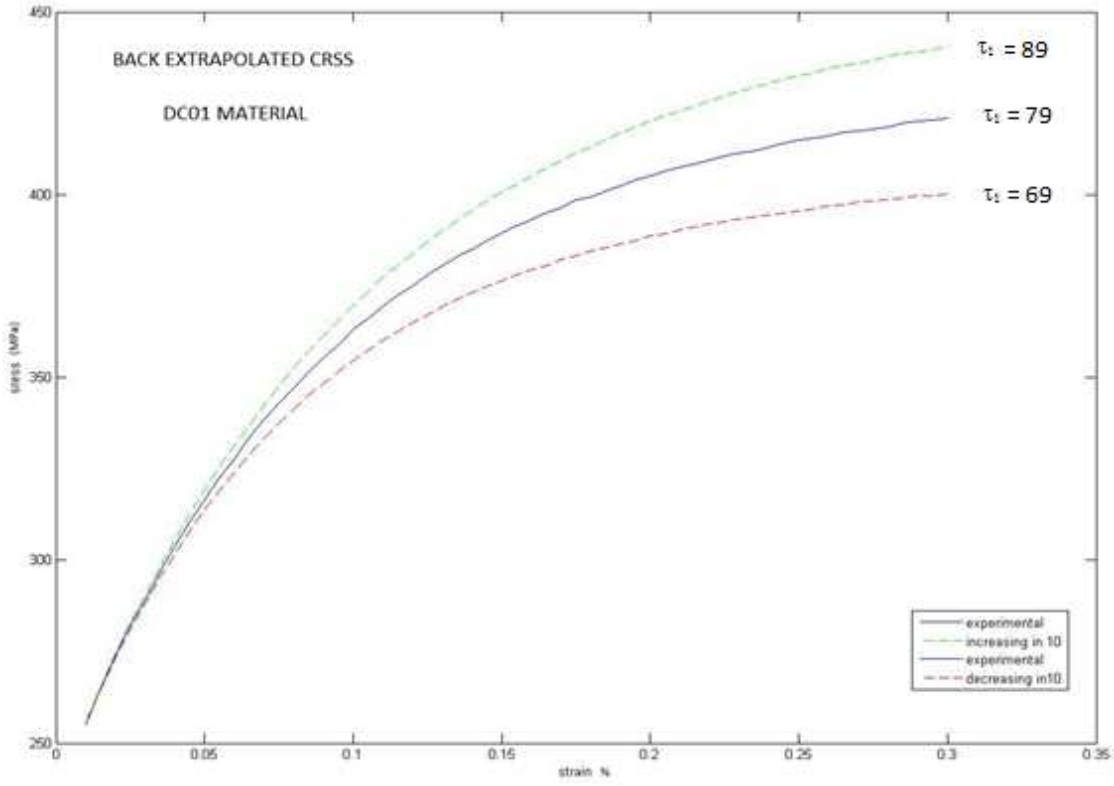

(a)

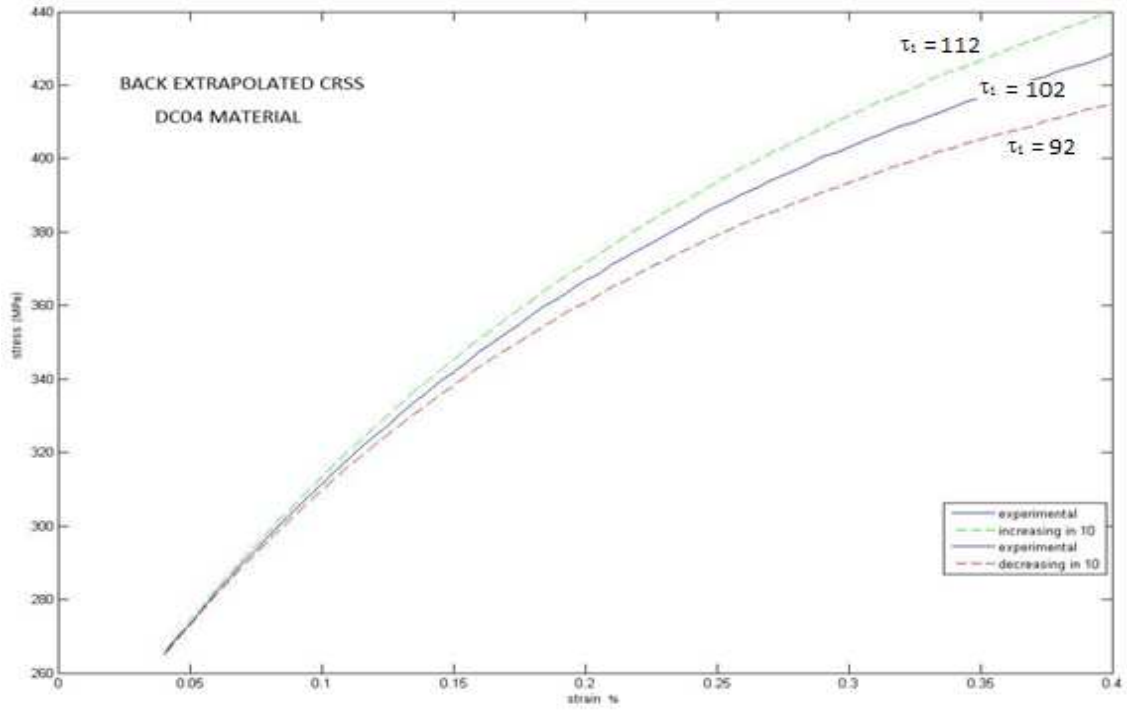

(b)

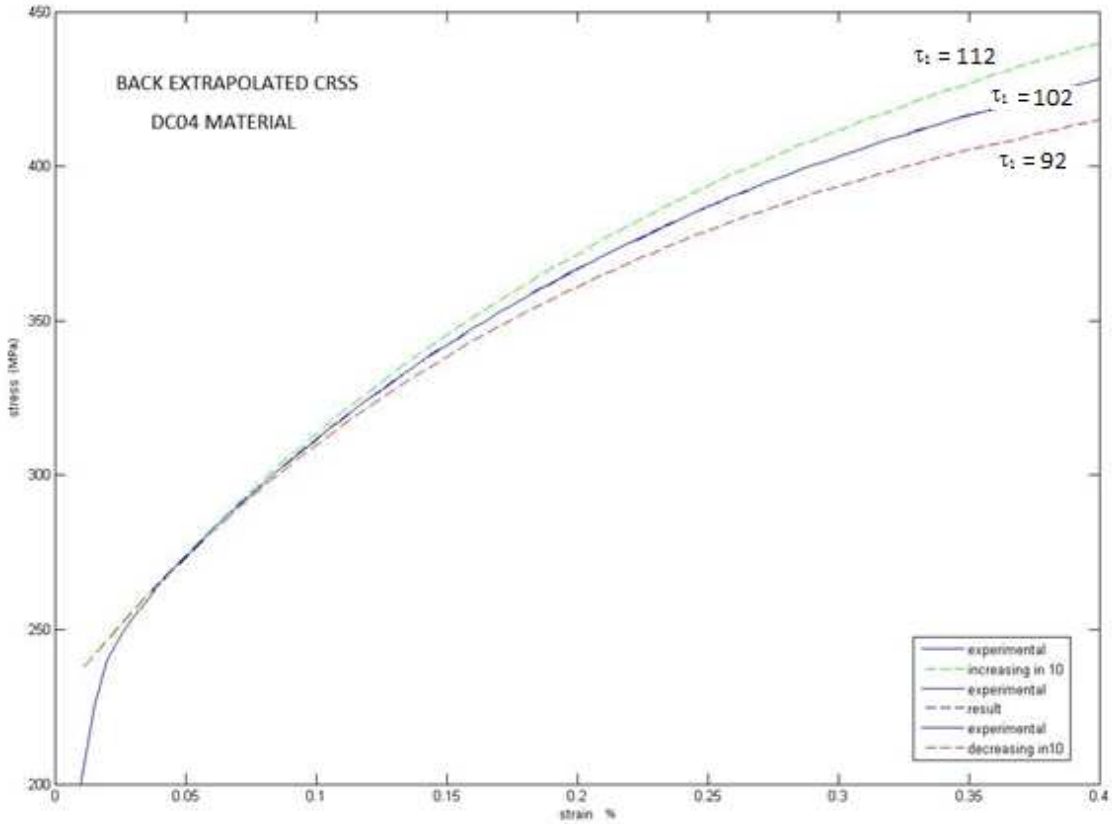

(c)

Figure 8.6 stress-strain curves for different τ_1 values. (a) DC01, (b) and (c) DC04.

8.5 ASYMPTOTIC HARDENING RATE

The parameter θ_0 has greatest influence on the arc of the curve, which is greater as θ_0 increases as we can see in Figure 8.7. However, the start and end points of the curves do not show dramatic differences between them. Comparing the results obtained from simulations with three different values of θ_0 can be seen as the hardening decrease and the yield stress point increase as asymptotic hardening rate increases.

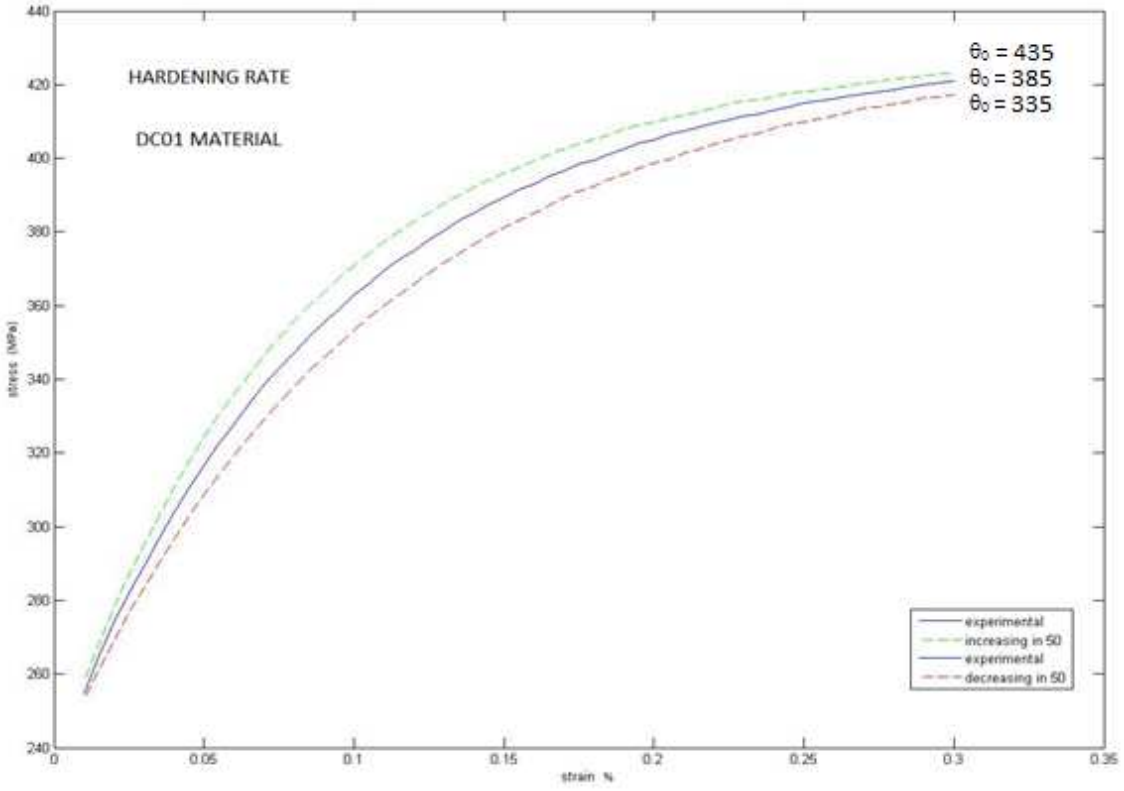

(a)

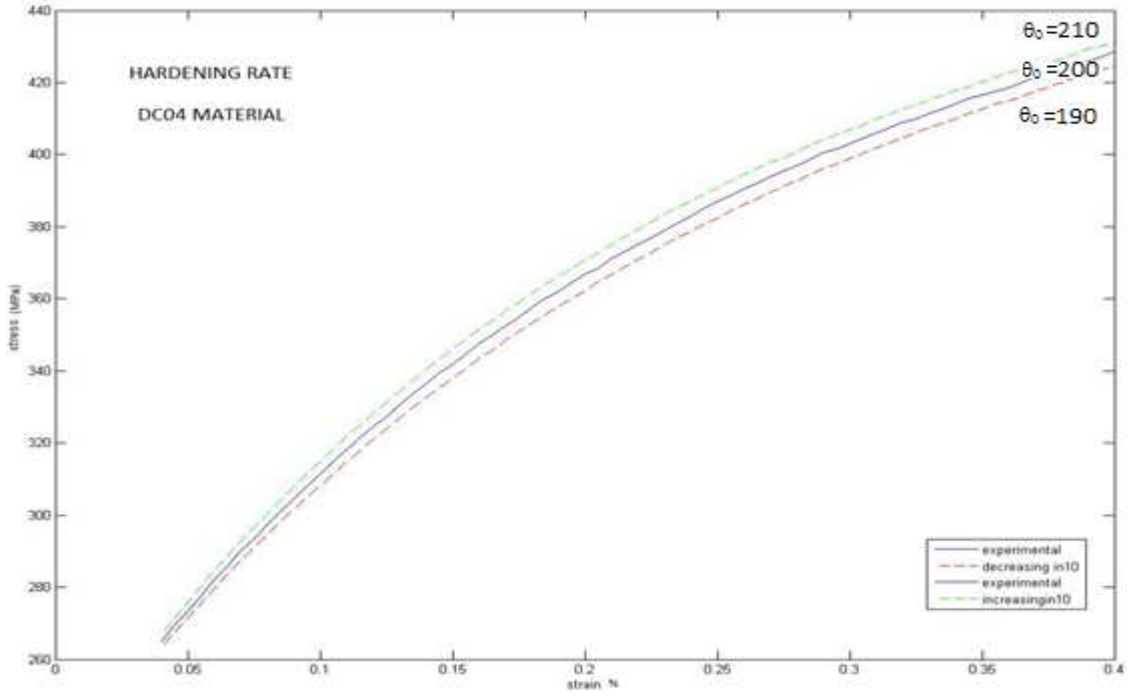

(b)

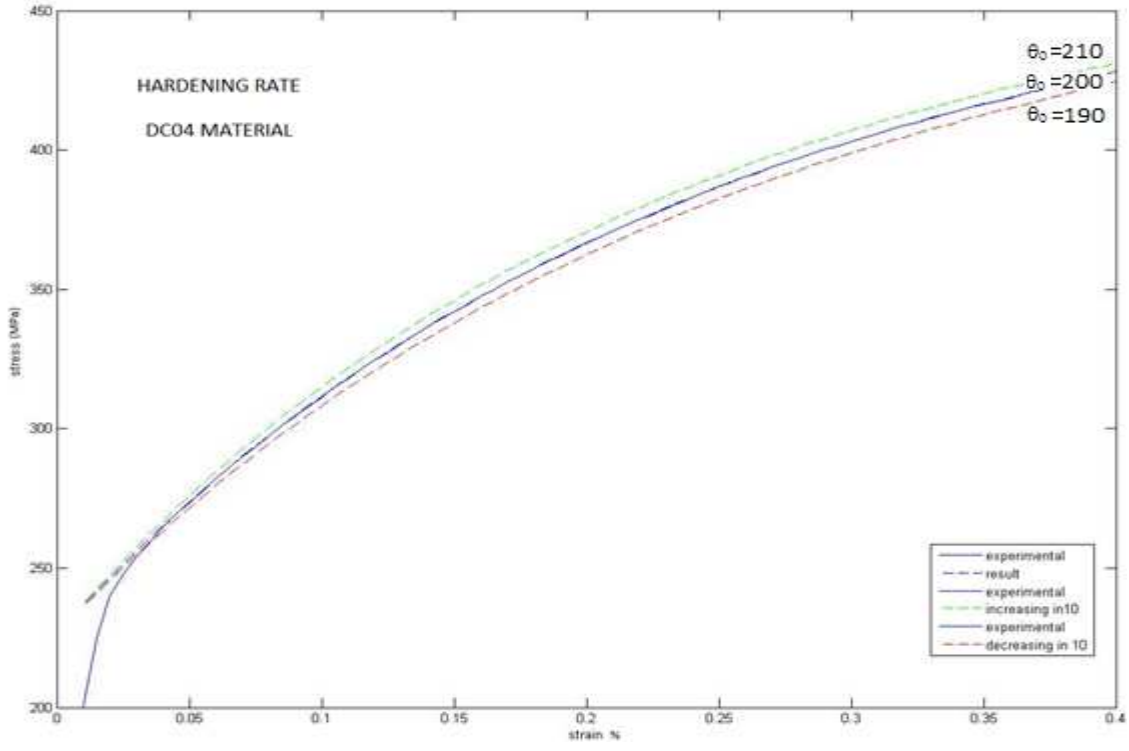

(c)

Figure 8.7 stress-strain curves for different θ_0 values. (a) DC01, (b) and (c) DC04.

8.6 MACROSCOPIC BEHAVIOUR

Deformation and slip in polycrystalline materials, as compared to single crystal is somewhat more complex due to the random crystallographic orientations of the numerous grains and the effect of neighboring atoms, the direction of slip varies from one grain to another.

In case of polycrystalline metals, greater stresses are required to initiate slip since they are stronger than their single crystal equivalents. This is also as a result of geometrical constrains that are imposed on the grain during deformation. It makes sense that as increase the hardening in single crystal due to the deformation process, the hardening in polycrystalline material increase as well.

Once we know the critical resolved shear stress and the strain mode we are able to obtain the equivalent stress and the equivalent strain since, as has been explain before, the Taylor factor equals the equivalent stress, relative to the critical resolved shear stress.

In order to measure the resistance of a material to a static or slowly applied force and the macroscopic behavior, a tensile test has been studied in which the material is deformed with a gradually increasing tensile load applied uniaxially along the long axis of the specimen. In tensile test the material is subjected to two different types of deformation; elongation along the tensile axis and contraction along the perpendicular direction as shown in Figure 8.8. ; So that it let us know important properties as when the yielding occurs, that is the stress level at which plastic deformation occurs, the yield strength or stress required to produce some amount of strain, the tensile strength that corresponds to the maximum stress that can be sustained by a material in tension and of course elastic properties as the modulus of elasticity.

The tensile test studied is obtained with the deformation gradient tensor in the form shown below, with epsilon, the strain rate.

$$\underline{\underline{F}} = \dot{\varepsilon} \begin{bmatrix} 1 & 0 & 0 \\ 0 & -0.5 & 0 \\ 0 & 0 & -0.5 \end{bmatrix}$$

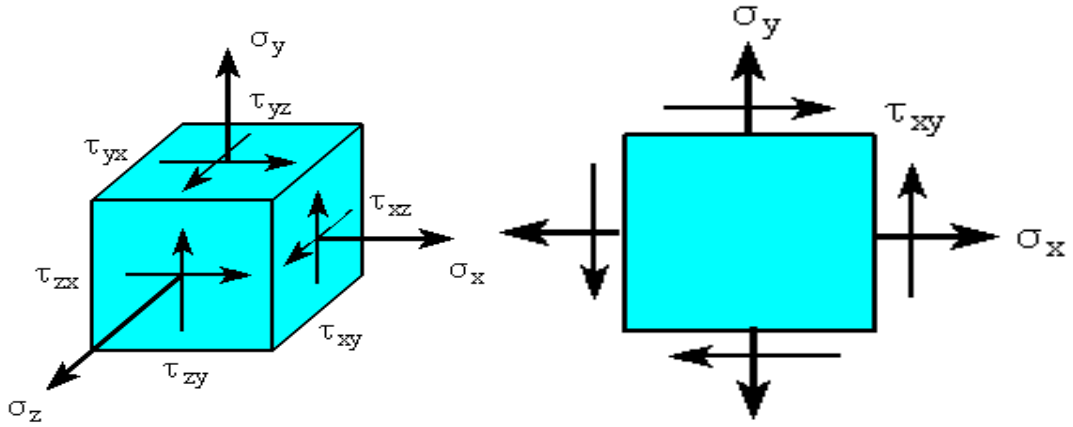

(a) (b)

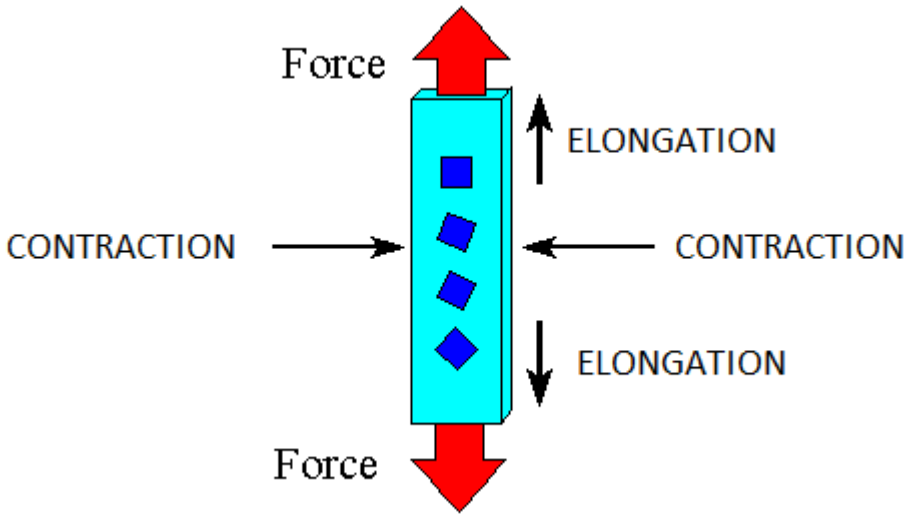

(c)

Figure 8.8(a) stresses representation (b) representation in plane stress ($\sigma_z = 0$) (c) Uniaxial tensile test

8.7 CONCLUSION

Due to plastic deformation both the grain shape and the dislocations arrangements change. Thus the grains are more elongated in the rolling direction as a consequence of dislocations movements and the dislocation density increase since new dislocations are created and must interact with that already existing. This phenomenon become more difficult for the dislocations to move through the existing ones and, thus the strain hardening consequently increase. It made sense to study the texture hardening since the grain structure has been deformed by work hardening once known that unlike the case in plane strain

compression, no single texture group could be identified to dominate over the plastic instability and flow localization process.

We know plastic deformation in real crystal is effected by successive movements of dislocations under the action of shear stress, thus critical resolved shear stress value has to be reached. In this work a set of material parameters need to be estimated by comparing simulation results to experimental stress-strain curves data. The two microscopic shear stress, τ_0 and τ_1 ,the asymptotic hardening rate θ_0 and the strain rate sensitivity *n*, are then adjusted to fit to the experimental curves for both cases.

Once known these parameters we will be able to predict the texture and anisotropy in rolling processes with Visco Plastic Self Consistent (VPSC) crystal plasticity model.

9 GENERAL CONCLUSIONS

The following conclusions can be draw from the present study:

First of all has been done a literature study of the texture evolution and the residual stress after cold rolling processes.

In this work, Visco Plastic Self Consistent (VPSC) model has been used in order to predict the texture, anisotropy and hardening development as well as the mechanical behaviour of a polycrystalline material after cold rolling process. Therefore has been necessary to calibrate the single crystal parameters, described by the Voce hardening law, based on the given tensile test.

The calibration procedure for the single crystal parameters has been done for two different kinds of steel, DC01 and DC04.This study has shown the influence of each of the parameters on the final stress-strain curve obtained using a single crystal Voce hardening law. The results of this study indicate that; the initial critical resolved shear stress (τ_0) influences directly the initial macroscopic stress value and does not influence the slope and consequently in the stress required to start and maintain the deformation in the material; The inverse of the rate sensitivity (*n*) parameter influences the initial stress value but unlike τ_0, *n* has an influence on the slope of the curve; The back extrapolated critical resolved stress (τ_1) allows to control the final stress value and the slope of the last part of the curve, therefore, it influence the

strength of the material in plastic deformation; Finally, the asymptotic hardening rate (θ_0) has a great influence on the curve, letting decrease the strength in plastic deformation .

Once the parameters are known they can be used as initial values in the optimization process in order to find the optimal parameters. Using the real parameters as an input in the VPSC polycrystal plasticity model that calculates texture evolution, anisotropy and hardening.The work was done in support of a fast material model to predict rolling forces and torques with online models.

The comparison between the simulations and experiments show the validity and usefulness of the approach, showing a good agreement in the DC01 case, and showing a small difference in the DC04 stress-strain graph in the first part.

Due to a lack of time, measurements of texture evolution and residual stress by means of X-ray diffraction have not been made.

10 REFERENCES

B. Beausir, L.S. Toth. "A new fliow function to model texture evolution in symmetric and asymmetric rolling ." *Microostructure and Texture in Steels 4*, 2009: 415-420.

B. Beausir, L.S. Toth, O. Bouaziz. "Simulation of texture development of plane carbon steel in miltipass rolling using analytical flow function." *Mat. Sc. Forum 495-497*, 2005: 1603-1608.

B. Verlinden, J. Driver, I. Samajdar. *Thermo-Mechanical Processing of Metallic Materials.* Elsevier, 2007.

Benoit Beausir, Laszio S Toth and Olivier Boaziz. "Simulation of texture development of plane carbon steel in multipass rolling using analytical flow function."

Bunge, HJ. *Texture Analysis in Material Science.* London: Butterworths, 1982.

CN. Tome, RA. Lebensohn. “VPSC7b Manual.” 2007.

Decroos, Koen. *The Influence of Anisotropy Due to Crystallographic.*

"DFG report."

Engler, Valerie Randle and Olaf. *Introduction to Texture Analysis : Macrotexture, Microtexture and Orientation Mapping.*

G. Totten, M. Howes and T. Inoue. *Handbook of Residual Stress and Deformation of sheet.*

Guinebretière, René. *X-ray Diffraction by Policrystalline Materials.*

J.Chakrabarty. "Theory of Plasticity." In *Theory of plasticity*, by J.Chakrabarty. 2006.

K. FEJA, V. HAUK and W. K. KRUG,L. PINTSCHOVIUS. *Residual Stress Evaluation of a Cold-rolled Steel Strip Using X-rays and a Layer.*

Kakani, S.L Kakaniand AmitT. "Material Science." In *Material Science*, by S.L Kakaniand AmitT Kakani.

L. Delannay, PJ. Jaques, SR. Kalidindi. “Finite element modeling of crystal plasticity with grains shaped as truncated octahedrons.” *Internatioinal Journal of Plasticity, Vol. 22, Issue 10*, 2006: 1879-1898.

L. PINTSCHOVIUS, V. HAUK and W. K. KRUG,. *Neutron Diffraction Study of the Residual Stress State of a Cold-rolled Steel.*

L.S. Toth, P. Gilormini, J.J. Jonas. "Effect of rate sensitivity on the stability of torsion textures." *Acta. Metallurgica 36*, 1988: 3077.

Lebensohn, Carlos N. Tomé and Ricardo A. *POLYCRYSTALPLASTICITY MODELING.*

Lebensohn, R. "VPSC." 1993.

M. Crumbach, G. Pomana, P. Wagner, G. Gottstein. "A Taylor type deformation texture model considering grain interaction and material properties. Part I – Fundamentals." *Gottstein, G., Molodov, D.A. (Eds.), Recrystallisation and Grain Growth, Proceedings of the First Joint Conference.* Berlin: Springer, 2001. 1053-1060.

Montmitonnet, Pierre. *Hot and cold strip rolling processes.*

Murty, K.G. *Linear programming.* New York: John Wiley & Sons, Inc, 1983.

R.A. Lebensohn, C.N. Tome. "A self-consistent anisotropic approach for the simulation of plastic deformation and texture development of polycrystals: application to zirconium alloys." *Acta Metall. Mater. 41*, 1993: 2611–2624.

T. Hoffmann, J .Kalisch ,A Bertram, S. Shim, J. Z. Tischler, H. Bei, B. C. Larson. "Experimental identification and validation of models in micro and macro plasticity."

T. Hoffmann, J. Kalisch, A. Bertram, S. Shim, J. Z. Tischler, H. Bei, B. C. Larson. *Experimental identification and validation of models in micro and macro.*

Taylor, G.I. "Plastic strain in metals." *J. Inst. Met. 62*, 1938: 307-324.

U. Kocks, C Tome, H. Wenk. *Texture and anisotropy: preferred orientations in polycrystals and their affect on materials properties.* Cambridge: Cambridge University Press, 1998.

UF. Kocks, CN. Tome, H. Wenk. *Texture and anisotropy: preferred orientations in polycrystals and their affect on materials properties.* Cambridge: Cambridge University Press, 1998.

Van Houtte, P. "Application of plastic potentials to strain rate sensitive and insensitive anisotropic materials." *Int. J. of Plasticity, 10(7)*, 1994: 719-748.

Van Houtte, P., L. Delannay, S.R. Kalidindi. "Comparison of two grain interaction models for polycrystal plasticity and deformation texture prediction." *Int. J. of Plasticity, 18(3)*, 2002: 359-377.

Van Houtte, P., S. Li, L. Delannay. "Deformation texture prediction: from the Taylor model to the advanced Lamel model." *Int. J. of Plasticity, 21(3)*, 2005: 589-624.

Van, M.Sc. Tung Phan. "Modeling the mesoscopic and macroscopic deformation behavior of the ferritic stainless steel DC04." In *Modeling the mesoscopic and macroscopic deformation behavior of the ferritic stainless steel DC04*, by M.Sc. Tung Phan Van.

Voce, E. "The relationship between stress and strain for homogeneous deformation." *J. Inst. Met. 74*, 1948: 537-562.